



**ADDIS ABABA UNIVERSITY
SCHOOL OF GRADUATE STUDIES
SCHOOL OF EARTH SCIENCES**

**PETROLOGY OF FLOOD VOLCANISM IN MERTULE MARYAM,
NORTHWESTERN ETHIOPIAN PLATEAU, CENTRAL ETHIOPIA**

**BY
BINIYAM FENTIE AYANA**

A thesis submitted to the School of Earth Sciences, graduate program, Addis Ababa University in partial fulfillment of the requirements for the degree of Master of Sciences in Geological Sciences (Petrology)

May 20, 2019

Addis Ababa, Ethiopia

**ADDIS ABABA UNIVERSITY
SCHOOL OF GRADUATE STUDIES
SCHOOL OF EARTH SCIENCES**

**PETROLOGY OF FLOOD VOLCANISM IN MERTULE MARYAM,
NORTHWESTERN ETHIOPIAN PLATEAU, CENTRAL ETHIOPIA**

**BY
BINIYAM FENTIE AYANA**

ADVISOR: DEREJE AYALEW (Prof.)

**A thesis submitted to the School of Graduate Studies of Addis Ababa University in
partial fulfillment of the requirements for the degree of Master of Science in Geological
Sciences (Petrology)**

**May 20, 2019
Addis Ababa, Ethiopia**

ADDIS ABABA UNIVERSITY
SCHOOL OF GRADUATE STUDIES
SCHOOL OF EARTH SCIENCES

**PETROLOGY OF FLOOD VOLCANISM IN MERTULE MARYAM,
NORTHWESTERN ETHIOPIAN PLATEAU, CENTRAL ETHIOPIA**

BY
BINIYAM FENTIE AYANA

Approved by the Examining Committee:

_____	_____	_____
Head, School of Earth Sciences	Signature	Date
_____	_____	_____
Advisor	Signature	Date
_____	_____	_____
Examiner	Signature	Date
_____	_____	_____
Examiner	Signature	Date

Declaration

I declare that this thesis is my original work under the supervision of Prof. Dereje Ayalew, School of Earth Science Addis Ababa University during the year 2018/19. I further declare that this work has not been presented or submitted to any other institution or university for the award of any degree or diploma. All sources and materials in the thesis work are well cited and dually acknowledged.

Biniyam Fentie Ayana

Signature

Date

This is to certify that the above declaration made by the candidate is correct to the best of my knowledge.

Prof. Dereje Ayalew (Advisor)

Signature

Date

Abstract

Mertule Maryam flood volcanism terrain is situated in the southern part of the northwestern Ethiopian plateau. The area is located 364 Km from Addis Ababa. The main objective of the thesis work is to understand the petrography and stratigraphy of Mertule Maryam area volcanic products and finally to assess the magmatic evolution. To accomplish the objectives, starting from the beginning various methods have been applied. The methods are; remote sensing, field observation, stratigraphy, petrography and geochemistry. The major volcanic units are plagioclase- pyroxene phyric basalt, agglomerate, aphyric basalt, plagioclase phyric basalt and undifferentiated aphyric basalt and tuff. The Mertule Maryam area volcanic products show narrow variation in composition of SiO₂ percentage (47.7 – 51 wt %) as mafic suits. Petrographic and stratigraphic observation of mafic samples from the study area suggested three divisions within the study area. These are dominantly plagioclase-pyroxene phyric, aphyric flow and plagioclase phyric flood basalt units. This distinctive petrographic heterogeneity reveals difference in depth of fractionation and magma flux in the lithosphere. The presence of plagioclase-pyroxene phyric basalt indicates there is considerable depth of fractionation in the shallow plumbing system. The aphyric basalt flow unit reflects there is no fractionation of any mineral in the shallow crust this indicates that the rate of magma flux to the shallow plumbing system is high. In addition the presence of plagioclase phyric basalt suggested that there was fractionation in the shallow plumbing system. Selected variation diagrams for major element and trace element shows scattered plot pattern which suggests these volcanic products are not the result of simple fractionation instead they do have different ways to come to the lithosphere.

Keywords: Ethiopian plateau, petrography, stratigraphy, phyric - aphyric texture, plumbing system, shallow crust, simple fractionation

Acknowledgement

I am glad to thank Jigjiga University for sponsoring me to attend my MSc program in Addis Ababa University. I am also thankful to Addis Ababa University, school of Earth Sciences, for delivering the required knowledge for the requirements of degree of masters in petrology.

My sincere and heartfelt gratitude goes to my advisor Prof. Dereje Ayalew for his help and guidance to complete my paper with in the time line of the academic calendar. He steered me in the right direction whenever I had troubles and problems in doing this paper from the start up to the end.

My gratitude also goes to Australian Laboratory Service (ALS) and Addis Ababa University petrographic laboratory professionals for geochemical data and thin section preparation. I heart fully acknowledge the people of Mertule Maryam locality for their hospitality, willingness and respectfulness to give necessary information during data collection.

From the beginning to the end of this research work I got lots of support from my friends, colleagues. Specially Mr. Amdemichael Zafu, Mr. Bahru Zinaye, Mr. Samuel Getachew, Mr. Abate Assen (Addis Ababa University), Takele Mengestie (Woldia University) and Tenaw Mengestie (Debre Berhan University) for their continuous encouragement, comments and multi-dimensional support to reach here. I have gratitude feeling to thank my family and friends my brothers, sisters and other persons not mentioned here for their unlimited support to complete my thesis work.

List of acronym

CFB – Continental Flood Basalt
Cpx -Clinopyroxene
DEM -Digital Elevation Model
EARS – East African Rift System
ERDAS - Earth Resources Data Analysis System
Fig. -Figure
GPS -Geographical Positioning System
HFSEs -High Field Strength Elements
HREEs- Heavy Rear Earth Elements
HT – High Titanium
LOI -Loss On Ignition
LREEs -Light Rare Earth Elements
LT – Low Titanium
MER – Main Ethiopian Rift
Mg# -Mg Number
My -Million years
NW – Northwestern
Plag – Plagioclase
PPL -Plane polarized light
Pxn – Pyroxene
SE – Southeastern
UTM - Universal Transverse Mercator
Wt% -Weight in percent
XPL -Cross polarized light

Table of Contents

Abstract.....	i
Acknowledgement	ii
List of acronym.....	iii
CHAPTER ONE.....	1
1. Introduction.....	1
1.1. Background.....	1
1.2. Geographic setting of the study area.....	3
1.2.1. Location and accessibility map of the study area.....	3
1.2.2. Physiography of the study area	4
1.2.3. Climate condition.....	4
1.2.4. Population and Settlement	5
1.3. Problem Statement	6
1.4. The objective of the research study.....	7
1.4.1. General objective	7
1.4.2. Specific objective.....	7
1.5. Methodology.....	8
1.6. Reviews of previous works	10
1.7 Thesis framework.....	12
CHAPTER – TWO	14
2. Regional Geological Setting	14
2.1. Introduction.....	14
2.2. The Cenozoic Ethiopian Volcanic Province	16
2.3. Northwestern Ethiopian Plateau Volcanics.....	19
2.3.1. The Oligocene Flood Volcanics (Trap Series).....	19
2.3.2. The Miocene - Pliocene Shield Volcanoes (Termaber Formation).....	21
2.3.3. Quaternary Volcanics.....	22
CHAPTER THREE	24
3. Geology of the study area	24
3.1. Introduction.....	24
3.2. Volcanic successions and petrographic descriptions	24
3.2.1. Plagioclase-pyroxene phyric basalt.....	27
3.2.2. Agglomerate.....	30
3.2.3. Aphyric basalt.....	32

3.2.4. Plagioclase phyric basalt	37
3.2.5. Undifferentiated aphyric basalt and tuff	41
3.2.6. Basaltic dike.....	43
CHAPTER FOUR.....	45
4. Whole rock geochemistry	45
4.1. Introduction.....	45
4.2. Chemical variation diagrams	49
4.2.1. Classification variation diagram	49
4.2.2. Major element variation diagram.....	50
4.2.3. Trace element variation diagram.....	51
4.3. Chemical Spider diagrams	56
4.3.1. Rare earth element spider diagram.....	56
4.3.2. Trace element spider diagram	57
CHAPTER FIVE	58
5. Discussion.....	58
5.1. Petrography	58
5.2. CIPW Normative minerals of Mertule Maryam volcanics	62
5.3. Petrogenetic indicators	63
CHAPTER SIX.....	65
6. Conclusion and Recommendation	65
6.1. Conclusions.....	65
6.2. Recommendations.....	66
REFERENCES	67
APPENDIX-A: Petrographic analysis results.....	72
APPENDIX-B: Selected trace element ratio of analyzed samples	74

List of figures

Figure.1.1. Cenozoic magmatic activity in Africa and parts of the Arabian Peninsula . .	2
Figure.1.2. Location and accessibility map of the study area.	3
Figure.1.3. A physiographic map of the study area	4
Figure.1.4. Bar charts showing climate and precipitation condition of.	5
Figure.1.5. Bar charts showing the population of Enebse sar midir Wereda.	6
Figure.2.1. Simplified geological map of Ethiopia and Eritrea	15
Figure.2.2. Schematic Illustration showing the Afar plume impinging on the Afro-Arabian lithosphere.....	18
Figure.2.3. Regional geological sketch map of Ethiopia plateau.....	23
Figure.3.1. Geological map of Mertule Maryam area flood basalt volcanism.....	25
Figure.3.2. Composite stratigraphic log section of Mertule Maryam area flood basalt volcanism.	26
Figure.3.3. Close up views of porphyritic basalt.	28
Figure.3.4. Microphotographs of plagioclase-pyroxene phyric basalt.....	30
Figure.3.5. close up views of agglomerate.....	31
Figure.3.6. Microphotographs of agglomerat..	32
Figure.3.7. Close - up views of aphyric basalt.....	33
Figure.3.8. Microphotographs of aphyric basaltic flow unit.....	34
Figure.3.9. Microphotographs of aphyric basaltic flow unit.....	35
Figure.3.10. Microphotographs of aphyric basalt unit.	36
Figure.3.11. Microphotographs of aphyric basalt unit.	37
Figure.3.12. close-up views of plagioclase phyric basalt.....	38
Figure.3.13. Microphotographs of columnar lava flow	39
Figure 3.14. Microphotographs of sparsely porphyritic lava flow.....	40
Figure.3.15. Microphotographs of plagioclase phyric basalt	41
Figure.3.16. Close-up views of weathered aphyric columnar basalt.	42
Figure.3.17. Microphotographs of aphyric basalt.	43
Figure.3.18. Microphotograph of a basaltic dike..	44
Figure.4.1. Total alkali-silica (TAS) diagram.....	49
Figure.4.2. Variation diagrams of selected major element	51
Figure.4.3. Variation diagrams of selected large ion lithophile (LIL) trace elements. ..	52
Figure.4.4. Variation diagrams of selected high field strength (HFS) trace elements. ..	53

Figure.4.5. Variation diagrams for compatible trace elements.	54
Figure.4.6. Variation diagrams for incompatible trace elements.	55
Figure.4.7, Spider diagrams of chondritic- normalized	56
Figure.4.8. Spider plot for trace element patterns normalized to the primordial mantle.	57
Figure. 5.1. Petrostratigraphy of Mertule Maryam area volcanic products	62

List of Tables

Table1.1. Summary of analytical procedures.....	10
Table1.2. Age data of different volcanic products from the northwestern Ethiopian	12
Table4.1. Geochemical data.....	46

CHAPTER ONE

1. Introduction

1.1. Background

The East African rift system is a particular interest because of having large Continental Flood Basalts (CFB) which erupted during the Paleogene period. The eruption is associated with regional uplift (of Ethiopian and Kenyan domes). These volcanics have been attributed to one or two distinct mantle plumes (Ebinger and Sleep, 1998; Rogers et al., 2000; Gezahegn Yirgu et al., 2006, cited in Beccaluva et al., 2009). The Ethiopian and Yemen Cenozoic flood basalt province is located at the junction of the three rifts that are formed during the breakup of Africa and Arabia. These are the Red Sea and the Gulf of Aden, both of which are floored by young mid-oceanic ridge spreading centers and the East Africa Rift where spreading remains confined to narrow continental volcano-tectonic zones (Furman et al., 2016). Continental flood basalt volcanism is often associated with rifting, as in the case of Afar- Red Sea – Gulf of Eden. The Ethiopian Cenozoic volcanic province constitutes one of the largest interplat magmatic provinces. These magmatic provinces are developed with the emission of a huge amount of flood basalt and interbedded ignimbrites (Pik et al., 1998; Dereje Ayalew et al., 2002; Beccaluva et al., 2009). The volcanic province of Ethiopia covers an area of greater than 600,000Km², is dominated by up to 300,000km³ of generally fissure-fed basaltic lavas forming the volcanic plateau bounding the Afar and Ethiopian Rifts (Mohr. 1983; Ebinger et al. 1993; Gezahegn Yirgu. 1997). These bounding plateaus are the southwestern and the northwestern Ethiopian plateaus.

The majority of flood basalt volcanism of Ethiopia has been erupted about 30My ago during a short 1 My or less time period to form enormous volcanic plateau (Hofmann et al., 1997 and Kieffer et al. 2004). Kieffer et al. (2004) suggested that immediately after this peak of activity a number of shield volcanoes are developed on the surface of the volcanic plateau.

According to Kieffer et al. (2004) and Beccaluva et al. (2009); the basalts in the Northwestern plateau are overlain by the shield volcanoes of tholeiitic (seimien shield) and alkaline lavas (Mt. Choke, Gugugftu, and Mt. Guna,). The southwestern part of the plateau is covered by alkaline lavas of Quaternary volcanic centers (Beccaluva et al., 2009). There are alkaline basalts and trachytes which were erupted in the Quaternary; those alkaline basalt

flows are characteristically the final pulse of basaltic volcanism on the Ethiopian plateau (Mengesha Tefera et al., 1996).

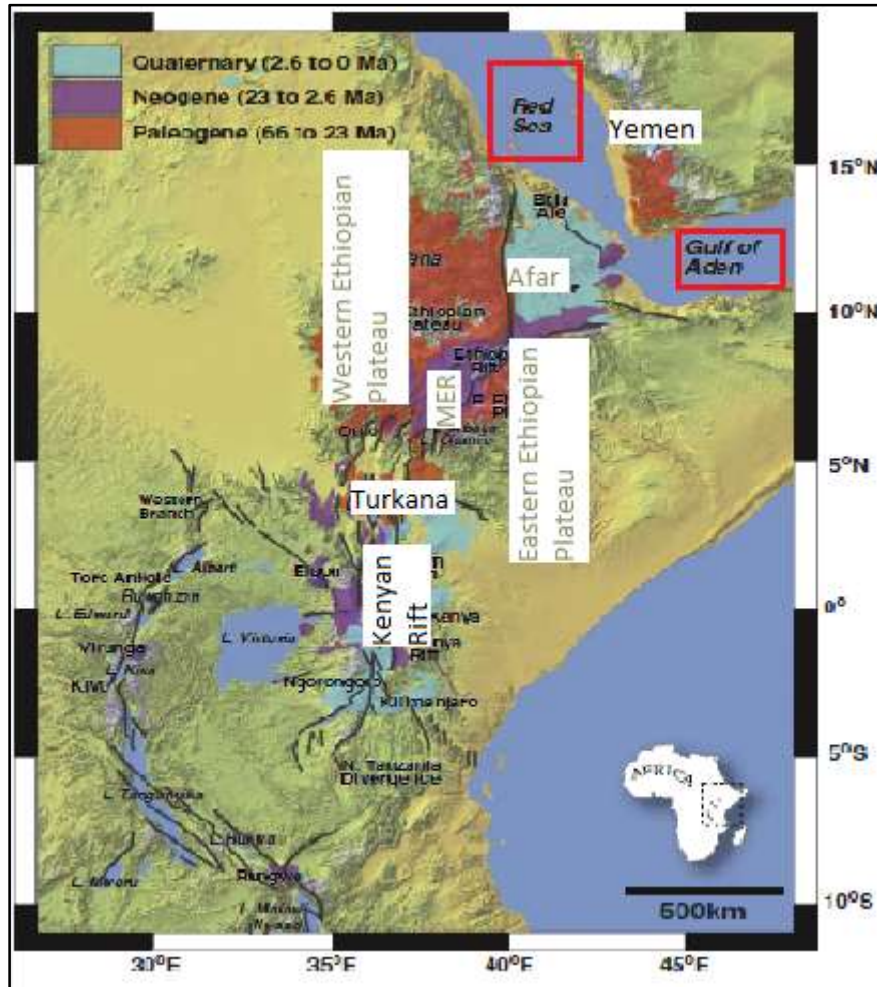


Figure .1.1. Cenozoic magmatic activity in Africa and parts of the Arabian Peninsula derived from the Geologic Map of Africa (Thiéblemont, 2016). Magmatic activity in East Africa is divided into three periods: Paleogene (66 to 23Ma); Neogene (23 to 2.6Ma); Quaternary (2.6 Ma to today). Major volcanic provinces are labeled. Background image is a colored SRTM (NASA) digital elevation model (PIA04965). Major faults, labeled as gray lines, are from Chorowicz (2005) Rooney (2017).

1.2. Geographic setting of the study area

1.2.1. Location and accessibility map of the study area

The study area is located in East Gojam Zone, Amhara National Regional State, Ethiopia. The area is accessible with Addis Ababa - Bahir-Dar main asphalt road. The traveling direction is from Addis Ababa – Dejene – Gundawyne - Mertule Maryam asphalt road; with a total distance of 364 km northwest of Addis Ababa. The research work is conducted in the northwestern plateau, north of central Ethiopia around Mertule Maryam that falls in the Deber Markos map sheet of the geological survey of Ethiopia. The area is bounded by a grid of Easting 0412000 and 0426000 and Northing 1195000 and 1205000 in UTM (Universal Transverse Mercator) coordinate system.

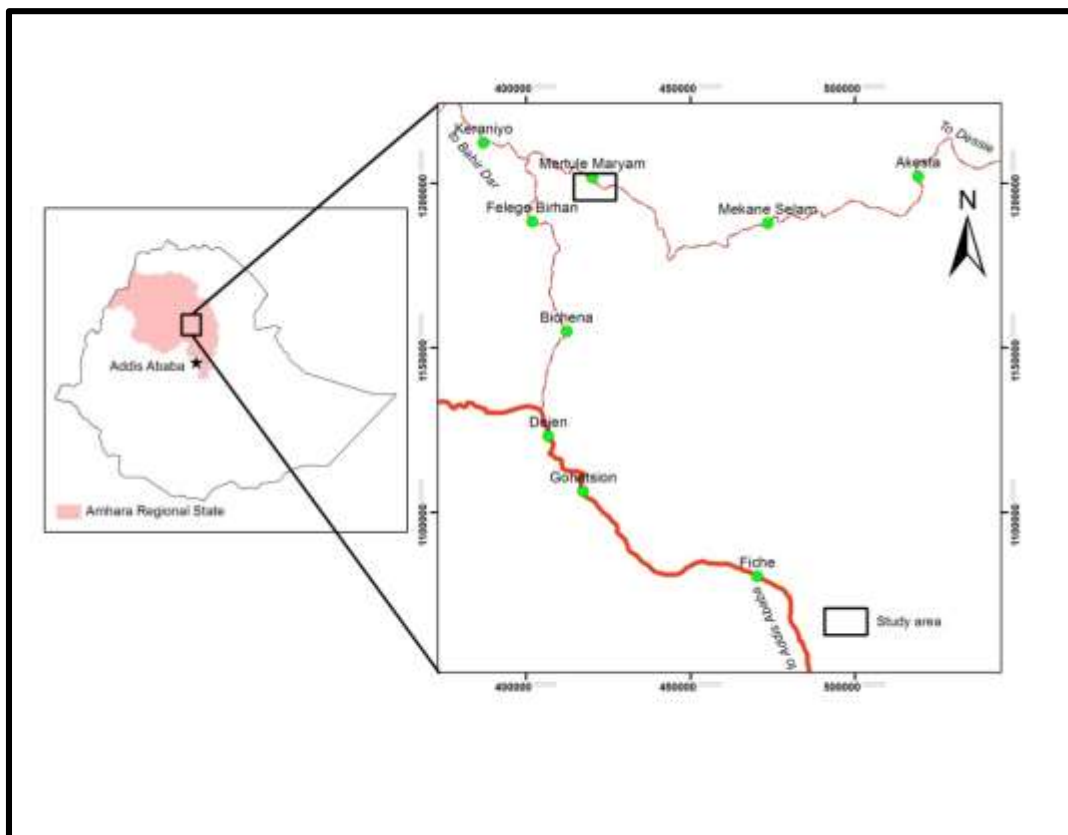


Figure.1.2. Location and accessibility map of the study area.

1.2.2. Physiography of the study area

The physiography of Ethiopia is divided into three due to the geological events that take place in geological history. These are the Main Ethiopian Rift (MER) and the Afar depression, northwestern Ethiopian plateau, and adjacent low lands and southeastern (Somali) plateau. The study area is the part of the plateau, located in the northwestern Ethiopian plateau. The vast volcanic and tectonic activity that took place after the flood basalt volcanism creates different physiographic features in the study area such as ridge, cliff and plains.

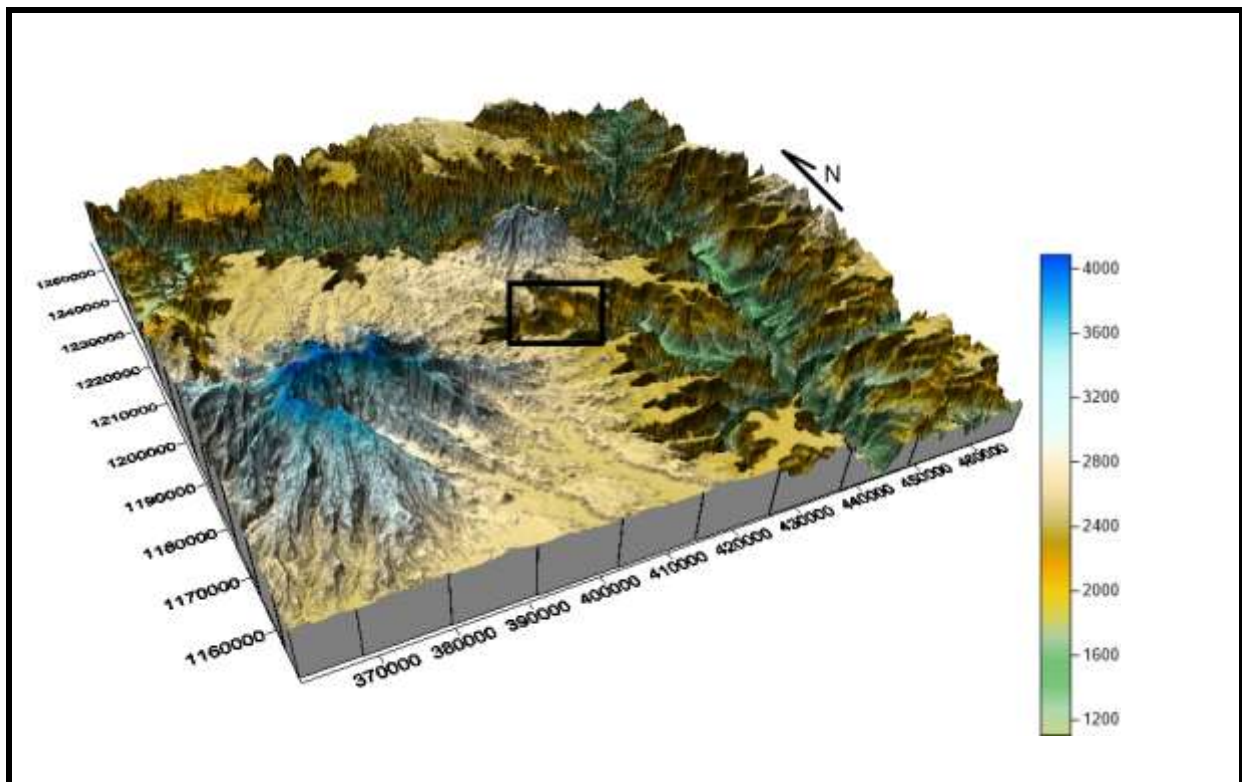


Figure.1.3. A physiographic map of the study area

1.2.3. Climate condition

The climate and weather condition in Mertule Maryam locality has intermediate temperature condition. The maximum and minimum average annual temperature of Mertule Maryam locality is range from 13.9 to 17.1 and its average annual precipitation also ranges from 11 to 348. The driest and the warmest months are January (11mm) and April (17.1.°c) respectively.

However, the wettest and the lowest temperature are recorded in July (348.mm) and August (13.9.°c) respectively and the variation in temperature and precipitation is 3.2.°c and 337.mm correspondingly.

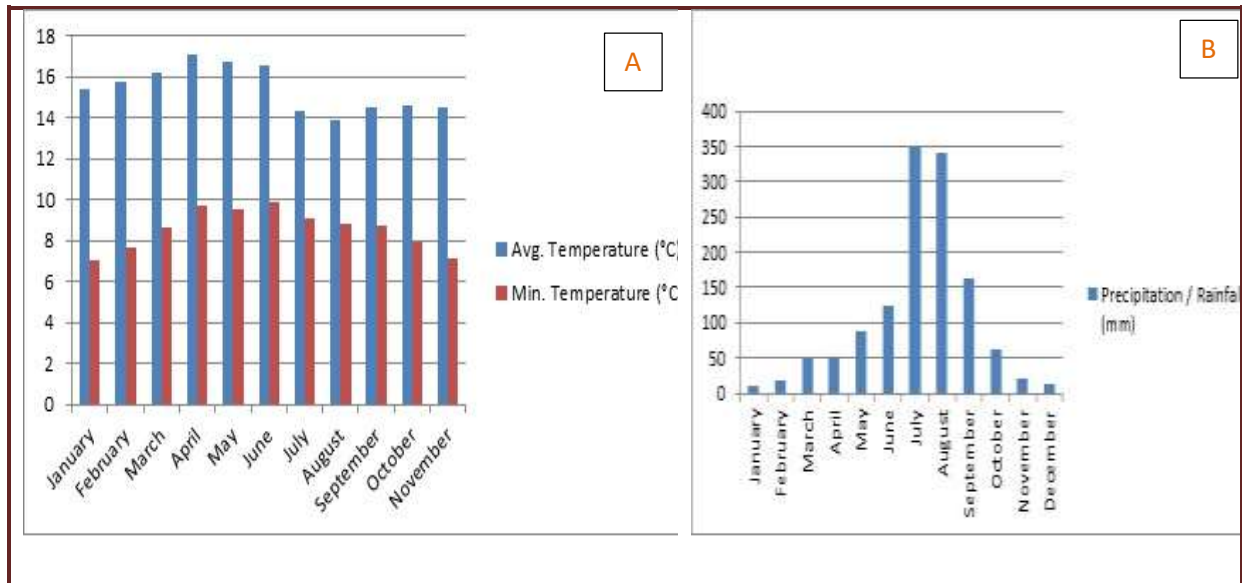


Fig.1.4. Bar charts, (A) showing climate and (B) precipitation condition of Mertule Maryam area, east Gojam. Sourced from Climate.data.org:[https://en.climate data.org/africa/ethiopia/amhara/mertule-mariam-928327/](https://en.climate.data.org/africa/ethiopia/amhara/mertule-mariam-928327/)

1.2.4. Population and Settlement

Based on the population census of 2007 conducted by the Ethiopian central statics agency (CSA) the total population of Enebse sar midir wereda, in which the study area is located, is 133,855. The Population density in the study area is generally low. Their livelihood is subsistence farming. Local peoples of the study area commonly cultivate some types of crops such as barley, maize, teff, and chickpea are the most common crops cultivated there.

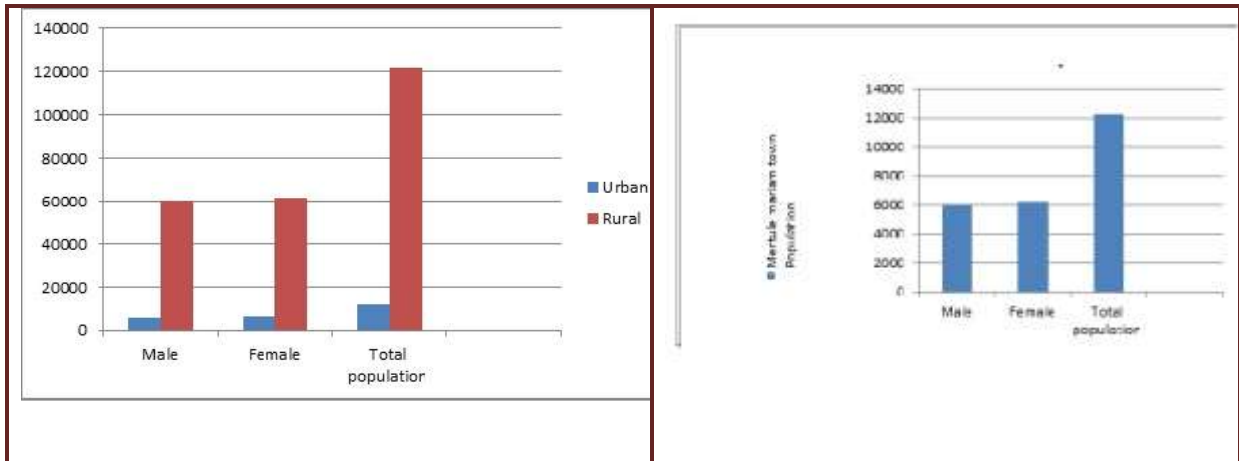


Figure.1.5. Bar charts showing the population of Enebse sar midir Wereda (left) and Mertule Mariam (right), east Gojam zone, Amhara regional state. The data source is from the 2007 Census conducted by the Central Statistical Agency of Ethiopia (CSA).

1.3. Problem Statement

In the northwestern Ethiopian plateau, many researches have been conducted on the flood basalt, shield volcanoes and quaternary volcanic products exposed in the plateau. The main Ethiopian rift divides Ethiopia into western and eastern plateaus that comprise the trap series (flood basalt) overlain by the complex shield volcanoes and quaternary volcanic products. Hence, this plateau is tectonically more stable; it gives complete geological record and conducting studies on the plateau volcanics give better geological evidence about volcanic history and magmatism of the area.

The continental flood basalts of Ethiopian plateau have been studied by many researchers (e.g., Mohr, 1983; George et al., 1998; Pik et al., 1998, 1999; Dereje Ayalew et al., 1999, 2002; Kieffer et al., 2004; Rooney 2017), some parts of Ethiopian flood basalt volcanic products like Mertule Maryam locality have been poorly understood from the evolution of the magmatic system. The trap series of northwestern Ethiopia basalts are divided into two; high titanium (HT) and low titanium (LT) geochemical group (Pik et al. 1998, 1999; Kieffer et al., 2004; Rooney., 2017). According to Pik et al. (1998), four localities were considered for their petrographic study (namely, Gonder, Adigrat, Lalibela, Blue Nile). Therefore, these cannot be considered as representative of the whole Northwestern Ethiopian plateau. The scientific gaps which are visible from previous studies on the present study area initiating to conduct this research are lack of detail geological map, stratigraphic log section,

petrographic, and geochemical data, assessments of the possible mode of formation and magmatic evolutions of volcanic products of the present study area.

Therefore, this study aims to fill these scientific gaps on petrology and petrography of the study area including: (i) to produce detail geological map of the study area (ii) producing stratigraphic log section of the volcanic products found in the study area (iii) sufficient petrographic studies for different lava flow types found in the study area, (iv) representative geochemical data analysis for major and trace elements signature and finally to understand the evolution of the magmatic system.

1.4. The objective of the research study

1.4.1. General objective

The general objective of this research work is to describe the petrography and stratigraphic succession of flood volcanism in *Mertule Maryam* area and finally to assess the evolution of the magmatic system.

1.4.2. Specific objective

- ❖ To produce a geologic map of the study area, that shows the distribution of volcanic products.
- ❖ To produce a composite stratigraphic log section of volcanic products and understanding the vertical succession of the lava flows.
- ❖ To recognize the mineralogical and petrographic features of volcanic rocks in Mertule Maryam locality; finally to assess their evolution, to recognize their relationship with the volcanic products found in the northwestern plateau.
- ❖ To characterize major and trace elements signature of rock suites in the study area and to assess the volcanic history by using different models like fractional crystallization, partial melting, and crustal contamination.
- ❖ To determine the eruption style of the volcanic products

1.5. Methodology

The overall framework of this thesis is categorized into three i) pre Fieldwork, ii) field work and iii) post-fieldwork.

i) Pre-fieldwork

In order to have an understanding on the magmatism, petrology, tectonic setting, volcanology and geochemistry of the study area all pertinent previous works on Ethiopian plateau have been assessed. The main Ethiopian rift valley and marginal volcanic products were systematically reviewed from published or unpublished reports, maps, journals, scientific publications and web sites, etc. These literature surveys used to have an understanding on the geological and geochemical data analysis, syntheses, presentation, and interpretation.

ii) Fieldwork and geological mapping

Fieldwork conducted with two phases to achieve the objective of this research work: the first phase for two consecutive days and the second phase for thirteen consecutive days. Field description of lavas, sampling and mapping was performed from December 28 up to January 11 to attain the objectives of this research work. Field traverse was selected principally for geological mapping, systematic sampling of different lava flows for petrographic description and geochemical analysis. During traverses, rocks were described at the outcrop level and photographs were taken at representative outcrops and structures.

In order to achieve this work base map, the application of remote sensing and GIS (ERDAS, and ArcGIS), Google Earth, Global Mapper, DEM and satellite images were used to produce location map, physiographic map and geological map of the study area.

iii). Laboratory and primary data

A. Petrographic analysis

The samples collected during fieldwork have prepared for two purposes: for petrographic study and for geochemical analysis. A Total of twenty-five fresh/free from alteration standard thin section samples were prepared in the mineralogy and petrographic laboratory of Addis

Ababa University. The descriptions of these thin sections are conducted in thin section preparation laboratory, School of Earth Science Addis Ababa University. Modal proportion, mineral identification, textural description, and rock naming were performed from data obtained with the petrographic study.

B. Analytical methods and sample preparation

A total of seven relatively fresh samples with free of alteration were analyzed by Australian Laboratory Service (ALS) laboratory service in Ireland. Samples were first crushed to 70% of < 2mm size and pulverized with a riffle splitter to have whole rock geochemical analysis. Pulverize split to 85% <75 μm and crushing tested with Quality Control (QC) test – pulverizing split tested with QC test. Geochemical data were generated using a combined method of Lithium Borate Fusion Inductively Coupled Plasma Emission Spectrometry (ICP-AES) analysis to determine major elements data; whereas, Inductively Coupled Plasma Mass Spectrometry (ICP-MS) was used to determine trace elements. From the analysis mentioned above the following major and trace elements are identified. Major elements SiO_2 , MgO , CaO , Fe_2O_3 , Al_2O_3 , Na_2O , TiO_2 , K_2O , P_2O_5 and MnO , analyzed with whole rock package ICP-AES (ME-ICP06) and trace elements are analyzed with whole rock package of Lithium Borate Fusion by ICP-MS(ME-MS81) such as Ba, Ce, Cr, Cs, Dy, Er, Eu, Ga, Gd, Hf, Ho, La, Lu, Nb, Nd, Pr, Rb, Sm, Sn, Sr, Ta, Tb, Th, Tm, U, V, W, Y, Yb, Zr. additionally, base metals Ag, As, Cd, Co, Cu, Li, Mo, Ni, Pb, Sc, Tl, Zn, analyzed with ICP-AES (ME-4ACD81) 4 acid digestions.

Table 1.1. Summary of analytical procedures

Analytical Methods/instruments	Australian laboratory (ALS) services code	Analyte	Descriptions
ICP-AES	ME-ICP06	Major elements	Whole rock package ICP-AES
WST-SEQ	OA-GRA05	Total volatiles	Loss on ignition at 1000 OC
ICP-MS	ME-MS81	Trace elements	Using lithium borate fusion ICP-MS
ICP-AES	TOT-ICP06	Major Elements	The total calculation for ICP06
ICP-AES	ME-4ACD81	Base metals	Using 4 acid digestions

1.6. Reviews of previous works

In East Africa Cenozoic plume-dominated magmatism extends from Turkana in the south, the southeastern Ethiopian plateau in the east, Yemen in the northeast, Ethiopia and Eritrea in the north, and Sudan in the west, and preserving a rich stratigraphic record of magmatism over the past 45 Ma (Rooney 2017; Krans et al., 2018). Basaltic magmatism is divided into three time periods: Eocene initial phase (45–34 Ma), Oligocene trap phase (~ 33.9–27 Ma), and the early Miocene resurgence phase (~ 26.9–22 Ma) which is later followed by bimodal lavas and silicic volcanism (Rooney 2017; Krans et al., 2018).

The Cenozoic volcanic rocks in Ethiopia can be subdivided in to trap series and Aden series. The term Trap Series is still widely used to refer to the whole pile of the Tertiary flood basalt sequence with intercalation of felsic lava and pyroclastic rocks in the uppermost units. The name Aden Series was used for post-rift volcanic rocks of the Main Ethiopian Rift, Afar Depression and some parts of the Ethiopian plateaus Mohr (1962 as cited in Mengesha Tefera et al., 1996).

According to Berhe et al.,(1987), Mohr and Zanettin., (1988), Tefera et al., (1996), Kieffer et al .,(2004), Rooney .,(2017); the volcanism of the northern and central part of western Ethiopian plateau subdivided in to four formations : the Ashangi basalt, Aiba fissural basalt, Alaji fissural basalts and rhyolites and Termaber basalts. Basically, this division is made based on lithologic or structural discontinuities between units.

Based on morphological boundaries the 1950-m thick Lima-Limo section found in the north of Lake Tana has been divided into upper and lower units. The lower 900-m thick section of lava capped by 150-m of differentiated products and an upper 1000-m thick section intercalated with silicic tuff (Hofmann et al., 1997; Krans et al., 2018). Subsequent research by Kieffer et al. (2004) assesses the transition from main phase low-titanium and high-titanium flood basalt through the development of shield volcanoes, including a lower 1470-m thickness of flood basalt and nearly 300-m of overlying shield volcanoes from three regions on the plateau.

Pik et al., (1998) conducted detailed geochemical studies on the Oligocene flood basalts of the northwestern Ethiopian trap series. The traps basalts grouped into three distinct geochemical groups based on Ti- concentration (low Titanium, High Titanium). Further, the high titanium basalts are sub-divided into HT1 and HT2. Based on this classification scheme, Mertule Maryam area volcanic products fall in the region of High-Titanium (HT1). The continental flood basalts province of Ethiopia (CFB) ~30 Ma, $3 \times 10^5 \text{ km}^3$ volume of flood basalt was formed as the result of the impingement of the Afar mantle plume beneath the Ethiopian lithosphere (Dereje Ayalew et al., 2002). Dereje Ayalew and Gezahegn Yirgu; (2003), recognized that the Ethiopian continental flood basalt province comprises a large volume of felsic eruptive rocks ($>6 \times 10^4 \text{ km}^3$) by volume overlying, and interlayered with the upper parts of the flood basalt sequence.

A number of large shield volcanoes were emplaced following the Oligocene flood basalt volcanism (Hoffmann et al., 1997; Kieffer et al., 2004). The northwestern Ethiopia shield volcanoes are magmatically similar to the underlying flood basalt, which is the tholeiitic Simien shield overlies tholeiitic flood basalts, and the alkaline Choke and Gugufu shields overlie alkaline flood basalts (Kieffer et al., 2004). Hofmann, et al., (1997), Coulie et al., (2001), Ukistins et al., (2002), Kieffer et al., (2004) provide absolute $40\text{Ar}/39\text{Ar}$ age determination on Oligocene-Miocene flood volcanics and Miocene -Pliocene volcanoes from the western Ethiopian plateau.

Kieffer et al., (2004) have been conducted on the petrology, geochemistry, and isotopic compositions of the large shield volcanoes, with the comparison of their compositions with those of the flood volcanics. These authors also traced the variations in eruption style and

magma flux of lavas with ages ranging from 30 to ~10 Ma, or from the peak of flood volcanism to the onset of major rifting in the northern part of the volcanic plateau.

Table 1.2. Age data of different volcanic products from the northwestern Ethiopian plateau (Hoffmann et al., 1997; Coulie., 2001; Ukstine et al., 2002; Kieffer et al., 2004, and reference therein)

Location	Age	Data source	Rock type
North of Addis Ababa	3.2-10.6Ma	Ukstine et al.,(2002)	Mio- Pliocene Volcano
Mt.Guna	10.7Ma	Kieffer et al.,(2004)	
Between Addis Ababa and Dese	10.9-11.7Ma	Ukstine et al.,(2002)	
Simien Mt.	18.7Ma	Kieffer et al.,(2004)	
Alem Ketema	21.6Ma	Coulie,(2001)	
Guguftu Mt.	22.3Ma		
Mt. Choke	22.4Ma		
Between Addis Ababa and Dese	25.3Ma	Ukstine et al.,(2002)	Flood Basalt
Blue Nile River	26.9-29.4Ma	Hoffmann et al.,(1997)	
Near Dese	25-30.9Ma		
WegeleTena	28.2-30.2Ma		
Lima Limo	29.4-30.8Ma		
Simien Mt.	30.4Ma	Kieffer et al.,(2004)	
Lalibela	31.0Ma		

1.7 Thesis framework

This thesis is framed with six chapters. The first chapter comprises of general background, location, accessibility, climate, population and settlement of the study area, problem statement, and objective of the study and research methods followed to achieve the study. An overview of the regional geological setting is presented in the second chapter. The geological map of the study area, composite stratigraphic log section, rock descriptions and petrographic investigations of analyzed samples are presented in chapter three. Chapter four presents the

geochemical data analysis, synthesis, presentations and interpretations using different geochemical models. Chapter five presents the discussion part of the thesis to summarize and generalize field, petrographic, and geochemical results, and interpretations. Lastly chapter six of the thesis deals on the conclusions on the stratigraphy and petrology of Mertule Maryam area flood basalt volcanism and recommendations for further study or points not covered in this research.

CHAPTER – TWO

2. Regional Geological Setting

2.1. Introduction

Ethiopia has one billion years of geologic history; this geological history can be divided into different geological time divisions: Precambrian, Paleozoic, Mesozoic, and Cenozoic. According to Mengesha Tefera et al., (1996) Ethiopia's physiography is divided into four major regions such as the western plateau, southeastern plateau, the main Ethiopian Rift and Afar Depression. However, the plateaus of Ethiopia is underlain by the Precambrian rocks of Afro- Arabian shield which is covered for the most part by Permian to Paleogene period; glacial and marine sediments, by tertiary volcanic and related sedimentary rocks. However, this volcanic succession was split apart by the Great East African Rift-System in Ethiopia.

In Ethiopia, the Precambrian rocks are exposed in the Northern, Western, Southwestern, and Southern and Eastern periphery of the country (Asfawossen Asrat et al., 2001). They consist of different variety of rocks such as: - sedimentary, volcanic and plutonic rocks which have been metamorphosed to varying degrees (Mengesha Tefera et al., 1996).

The Precambrian basement rocks of Ethiopia are related to the east African orogeny, and this orogeny has two distinct sections with relatively different rock types. These are the Arabian-Nubian Shield (ANS) and Mozambique Belt (MB), which are exposed in the northern and southern part of the country respectively (Williams, 2016). According to Abbate et al., (2015), in northern Ethiopia the ANS dominantly comprises low-grade metavolcanic-volcanoclastic rocks overlain by metasedimentary rocks. Whereas in southern Ethiopia the MB consists of amphibolites, granulite facies metamorphic rocks and gneiss terrains are abundant.

The Paleozoic era in Ethiopia is recognized by regional unconformity due to widespread erosional processes (denudation), which reduce the mountains formed by the Precambrian crystalline basement into peneplain (Williams, 2016). However, there is also very few deposits which were formed during this era such as, tillites which is found in several

localities mainly in the northern Ethiopia together with layers of sandstone and Ordovician to Silurian fluviatile lower Enthicho sandstone which is overlain by late Carboniferous to early Permian upper Enticho sandstone and Edaga Arbi Glacials (Abbate et al., 2015).

According to Abbate et al., (2015), the Mesozoic era is recognized by the transgression and regression of the Indian Ocean in East Africa and Ethiopia. Subsequently, this event has created a different type of sedimentary rocks in different parts of the country such as in North (Mekele Basin), in central Ethiopia (in the Abay Basin), and in southeastern Ethiopia (Ogaden Basin). The process resulted in the deposition of fluviatile sandstones and associated siltstones, sub-continental and marine deposits comprised of shales, marls, dolomite, gypsum, clay, limestone and sandstone inter-bedded with silt, mudstone shale, laterite, and conglomerates. The Cenozoic era is recognized by extensive volcanic activities and continental rifting in East Africa and Ethiopia. In Ethiopia, the Mesozoic sediments and the Precambrian basement rocks are covered by flood basalt volcanism which is overlain by shield volcanoes of Miocene age, Quaternary volcanics and sedimentary deposits.

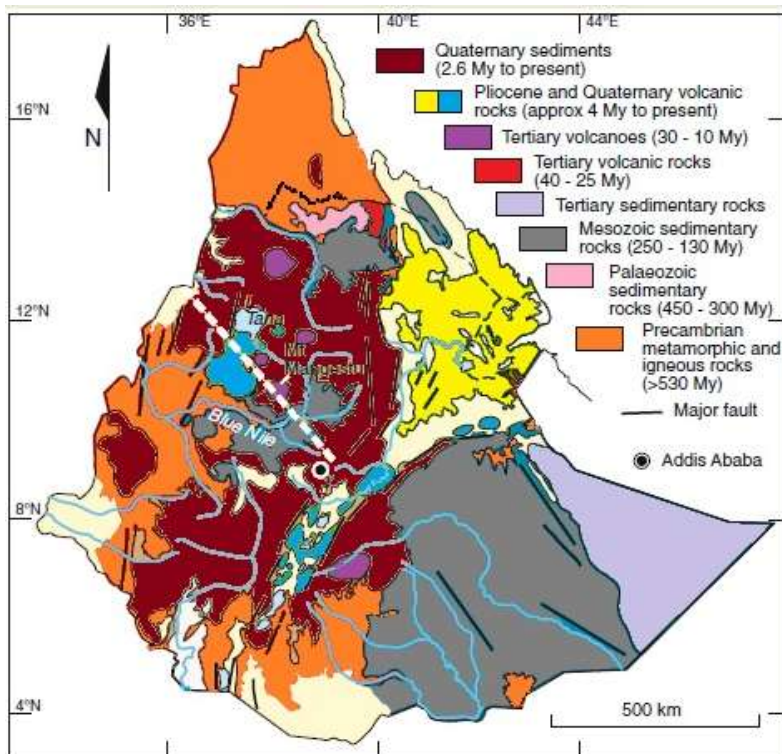


Figure.2.1. Simplified geological map of Ethiopia and Eritrea (After Williams, 2016)

2.2. The Cenozoic Ethiopian Volcanic Province

Magmatic activity in the Cenozoic era has been initiated 45Ma in the Southern Ethiopia with the eruption of Amaro basalts over the Mesozoic sediments, which, is underlain by the Precambrian crystalline basement (Ebinger et al., 1993 and Rooney, 2017). Following this, the second phase of magmatism in East Africa is concentrated on the NW Ethiopian plateau and the earlier contiguous portion of Yemen (Rooney, 2017). The Cenozoic continental flood basalts (CFB) of Ethiopia are located at the junction of the three rift system Red Sea, Gulf of Aden and the East Africa continental rift system. The majority of the province crops out in Ethiopia while the rest of the province is exposed in the eastern side of the Red Sea (Pik et al., 1998).

The Basaltic magmatism is divided into three time periods: Eocene initial phase (45–34 Ma), Oligocene trap phase (~ 33.9–27 Ma), and the early Miocene resurgence phase (~ 26.9–22 Ma) which is later followed by bimodal lavas and silicic volcanism (Rooney, 2017 and Krans et al., 2018). Eocene initial phase volcanism is dominantly basaltic and this basaltic volcanism was restricted to southern Ethiopia and northern Kenya (Furman et al., 2006; Rooney, 2017; Krans et al., 2018). During the Oligocene, the eruption of the Ethiopian Arabian plateau flood basalt takes place over north Ethiopia and Yemen with a significant areal extent of volcanism (Baker et al., 1996; Hofmann et al., 1997; Rooney, 2017). During the Miocene resurgence phase basaltic activity occurred in the form of shield activity in the northwestern Ethiopian plateau, fissure eruption on the southeast plateau and increased eruptions in the Turkana region (Kieffer et al., 2004; Furman et al., 2006; Rooney, 2017; Krans et al., 2018). Mohr and Zanettin (1988) suggested a four-fold division of the trap basalts of Ethiopia such as Ashangi basalt, Aiba fissural basalt, Alaji fissural basalt and rhyolite, and Termaber basalt.

Ashangi basalt: is the lowest unit on the northwestern Ethiopia which is characterized by altered flood basalt which was tilted up to 40° and this flood basalt is common in central Ethiopia.

Aiba fissural basalt: this flood basalt unit uncomfortably overlies the ashangi basalt unit; the flows of this unit are 15-50 m thick and it shows a columnar nature.

Alaji fissural basalt and rhyolite: this unit is an intercalated basaltic and rhyolite unit which is the final stage of flood basalt volcanism and the thickness of the flows is about tens of meters.

Termaber - Megezez formation: this is the last division of the trap basalts which is more localized basalt that overlies the alaji basalts and rhyolites. They are fissure fed low angle shield volcanoes.

The above classification is from some stratigraphic sections in the Ethiopian plateau; hence this classification is not valid for the entire volcanic products of the plateau (Beccaluva et al., 2009). However, a new major and trace element analysis of basalts from the northwestern Ethiopian plateau confirms the existence of three main magma types subdivided based on the concentration of TiO_2 (Pik et al., 1998). According to Pik et al., (1998); the northwestern Ethiopian plateau basalts are subdivided into high-titanium (HT) and low- titanium (LT). The northwestern plateau high-Ti flood basalts have a distinctive geochemical domain that is characterized by transitional basalts with $\text{Ti/Y} > 450$ and $\text{Nb/Y} > 0.45$. Further, the HT flood basalts are subdivided into HT1 (relatively lower Ti/Y and Nb/Y) and HT2 group with higher values of ratios ($\text{Ti/Y} > 700$ and $\text{Nb/Y} > 0.90$). The low titanium basalts are transitional to tholeitic and characterized by low TiO_2 and high SiO_2 (Pik et al., 1998 and Rooney, 2017).

The formation of the trap series is followed by the initiation of the Main Ethiopian Rift (MER). The MER is an important segment of the East African Rift System (EARS), which constitutes north most part of the EARS that connects the EARS with Afar triple junction (Bekele Abebe et al., 2007 and Corti, 2009). The MER is a magmatic rift that records all the different stages of rift evolution. As a result, it is an ideal place to analyze the evolution of continental extension and the rupture of lithospheric plates (Corti, 2009). Corti (2009) noted that physiographically the main Ethiopian rift can be divided into three segments southern, central and northern segments.

The MER is bounded by discontinuous boundary fault that separates the rift depression from the western (Ethiopia) and eastern (Somalia) plateau. These boundary faults are characterized by long, widely spaced and large vertical offset $> 1\text{-km}$ (Boccaletti et al., 1998 and Corti, 2009).

Volcanism in the MER is mainly characterized by bimodal composition volcanism of basalts and rhyolites, with distinct lack of lava of intermediate composition (Peccerillo et al., 2003

and Bekele Abebe et al., 2007). According to Bekele Abebe et al. (2007) in the MER two main Quaternary magmatic episodes are recognized. These are basaltic flows followed by ignimbrites and silicic centers in the rift floor (2 – 1 Ma) and axial silicic volcanoes and basalts since ~650.Ka. The first episode of magmatism comprises mainly basaltic flows and scattered silicic centers developed along the rift floor.

In northern Ethiopia and the conjugate Yemen margin, CFB generation was favored by several factors: 1) lowered solidus temperatures of plume metasomatized mantle sources; 2) heat transfer by the plume buoyancy flux that raised the regional geotherm; and 3) decompression of the upwelling mantle (Beccaluva et al., 2009).

Cenozoic flood basalt volcanism, plateau uplift, and the development of the Main Ethiopian and Afar rift systems have been attributed to the upwelling of a mantle plume with a potential link to the African Super- plume (Pik et al., 1998, Kieffer et al., 2004).

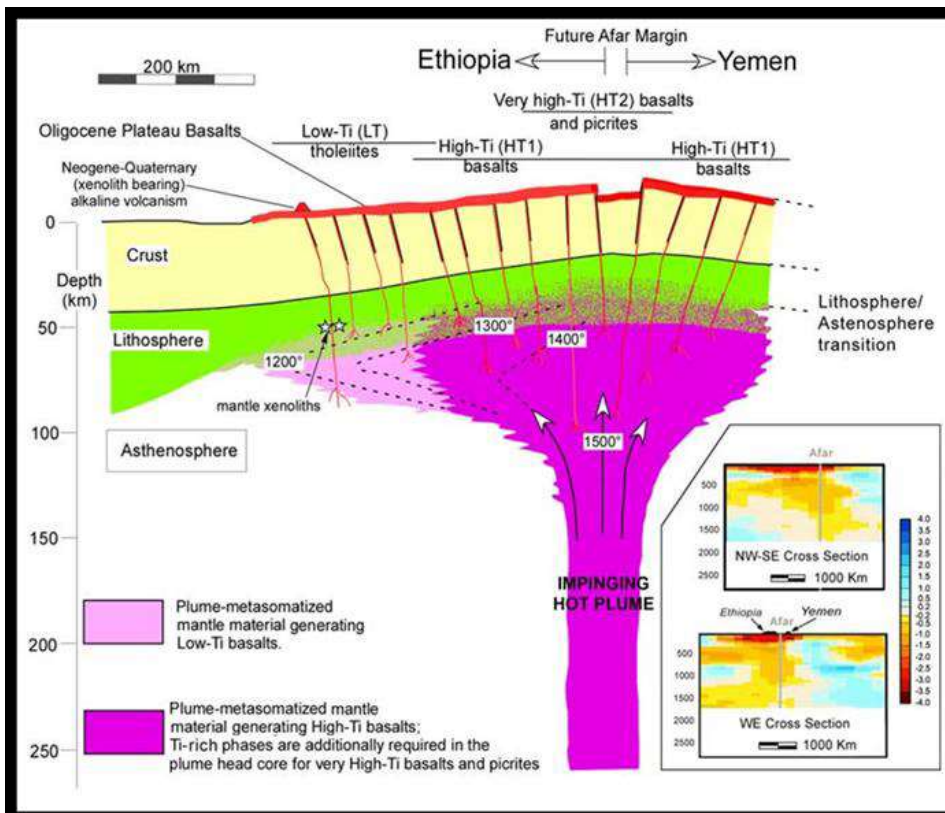


Figure.2.2. Schematic Illustration showing the Afar plume impinging on the Afro-Arabian lithosphere and the generation of Oligocene Northern Ethiopia-Yemen CFBs from a thermally and compositionally zoned plume head (Beccaluva et al., 2009) The inset shows mantle tomographic cross-sections beneath Afar, based on models for shear-wave velocity variations (Davaille et al., 2005).

2.3. Northwestern Ethiopian Plateau Volcanics

The volcanic succession of Ethiopia is cut into two major sectors as northwestern (Ethiopian) and southeastern (Somalia) plateau by the Ethiopian Rift. The western plateau includes the northern, central, and southwestern sectors, whereas the southeastern plateau comprises the eastern, southeastern and southernmost part of the Ethiopian flood volcanic province (Corti, 2009).

The volcanic succession in the northwestern Ethiopian plateau is emplaced on the horizontal to subhorizontal transgressive and regressive sedimentary strata of Mesozoic age. However this volcanic plateau does not fit the popular image of a continental flood basalt province in that it is not a thick, monotonous, quickly erupted pile of flat – laying tholeiitic basalt. Instead, it consists of a number of volcanic centers with different age and magmatic character (Kieffer et al., 2004).

The northwestern traps comprise a series of late Eocene and Oligocene fissure basalts, covered by Miocene shield volcanoes. It has a conventional K/Ar age range of 14 to 140 Ma which is measured from basalts, rhyolites and ignimbrites from the plateau to the north of Addis Ababa (Hofmann et al., 1997).

According to Kieffer et al., (2004) the northwestern Ethiopian plateau volcanic units have mainly classified as the Oligocene flood volcanics (trap series) comprised of Oligocene – Miocene basalts and rhyolites, the Miocene –Pliocene shield volcanoes, volcanic plugs and domes, and Quaternary volcanics.

2.3.1. The Oligocene Flood Volcanics (Trap Series)

In Ethiopia, the flood basalts (traps) cover an area of about 600,000-km² with different layers of felsic and basaltic volcanic rocks. The thickness of these layers of basaltic and felsic volcanic rocks are highly variable in different regions however, it reaches 2000.m in some regions. Further, the total volume of volcanic and shallow intrusive rocks has been estimated about 350,000-km³ (Mohr, 1983, Mohr & Zanettin, 1988 and Kieffer et al., 2004).

The northwestern Ethiopian Oligocene volcanism has been traditionally subdivided into two formations based on chrono-stratigraphy (Berhe et al., 1987; Pik et al., 1998); these are the Ashangi and Aiba basaltic units, separated by an angular unconformity (Zanettin et al., 1980 as cited in Pik et al., 1998) and the upper ignimbritic Alaji unit. This classification is based on a few sections of the northwestern plateau; therefore; this stratigraphic classification is not valid for the entire plateau (Pik et al., 1998). Pik et al., (1998) suggested that the northwestern Ethiopian plateau is composed of continuous lava sequence from the base to the top of the plateau, rather than the piling of successive and stratigraphic distinct units.

However, the lava sequence of the northwestern Ethiopia plateau subdivided into two different groups of lava such as low titanium (LT) and high – titanium (HT). Low – titanium basalts are characterized by relatively flat rare earth element (REE) pattern and low level of Ti and incompatible trace elements (Pik et al., 1998, 1999; Kieffer et al., 2004; Beccaluva et al., 2009). Pik et al., (1998) and Kieffer et al., (2004) suggested that high titanium (HT1 and HT2) basalts are characterized by a higher concentration of incompatible trace element and more fractionated rare earth element pattern. However, HT2 basalts are slightly more magnesian than the HT1 basalts and these basalts are rich in olivine ± clinopyroxene phenocrysts. They also have a higher concentration of incompatible trace element and extreme fractionation of rare earth element than HT1 basalts.

Most of the northern Ethiopia trap series has yielded an age $30\text{Ma} \pm \text{few Ka}$ from $^{40}\text{Ar}/^{39}\text{Ar}$ dating (Hoffmann et al., 1997; Coulie et al., 2003; Kieffer et al., 2004). Different basaltic sections were examined for dating of the flood basalts in the northwestern Ethiopian plateau by using the $^{40}\text{Ar}/^{39}\text{Ar}$ technique. Accordingly, the basalts from Lima Limo and Wegel Tena section yielded age of 30.8 to 29.4-Ma and 30.2 to 28.2-Ma respectively (Hoffmann et al., 1997), further investigation of basalt from the central section of the northwestern Ethiopian plateau, along the Woreta- Woldia which yielded a plateau age of 29.6 to 29.2-Ma and 30.4-Ma at the base of the Adigrat section, the other section that shows 29.4 to 26.9-Ma is the Blue Nile Valley basalts that overlay on the Mesozoic sediments.

In addition to the Oligocene flood basalts, the western plateau of Ethiopia comprises of Oligocene ignimbrite deposits. These Oligocene - ignimbrites cover an area of $7 \times 10^4 \text{ km}^2$ with an estimated volume of $4.3 \times 10^4 \text{ km}^3$, it represents an average of 20% of the volcanic pile. Oligocene rhyolites are outcropped in three geographically distinct regions in the

western plateau of Ethiopia such as Lima Limo rhyolites in the northwestern plateau forming several beds overlying the LT flood basalts, Wegel Tena rhyolites in the east corresponding to thick ignimbrite and Jima rhyolites located in the southwestern plateau overlying on the high- titanium flood basalts (Dereje Ayalew et al., 2002).

2.3.2. The Miocene - Pliocene Shield Volcanoes (Termaber Formation)

The flood volcanism is followed by the emplacement of large shield volcanoes and the development of continental rift (Mohr., 1983; Hoffmann et al., 1997). The thick succession of the flood basalt is overlain by a number of large shield volcanoes which are developed on the surface of the volcanic plateau (Kieffer et al., 2004). These shield volcanoes are conspicuous features of the Ethiopian plateau and they are also the distinguishing features of Ethiopian plateau from other flood basalt provinces such as Deccan and Karoo. Currently, about 20% of the surface of the plateau is covered with shields, the summit of the shields are 1.5 km above the flood basalt with the volume of 20% of that of the flood basalts that are about $4 \times 10^4 \text{ km}^3$ (Kieffer et al., 2004).

Choke and Gugufu shields are the manifestations of shield volcanoes developed on the surface of the northwestern Ethiopian plateau. Choke which rises over 4000m in elevation and has a basal diameter of 100km and Gugufu which rises to ~3900 m (Kieffer et al., 2004; Rooney 2017). The magmatic activity which makes up Choke and Gugufu is thinner and less continuous similar to the Oligocene Simien shield, but these shields are more alkaline than the underlying flood basalts (Kieffer et al., 2004; Rooney, 2017).

A basaltic sample at the base of choke yielded $^{40}\text{Ar} - ^{39}\text{Ar}$ age of 23 Ma (Kieffer et al., 2004; Rooney 2017), Moreover from $^{40}\text{Ar} - ^{39}\text{Ar}$ dates on the rhyolites the upper limit of magmatism at Choke and Gugufu are 22.4 and 23.3 Ma respectively the other shield which is located between Simien and Choke is Mt Guna that provides an age of 10.7 Ma (Kieffer et al., 2004).

These volcanoes are characterized by more porphyritic texture containing abundant phenocrysts of plagioclase and olivine. They are mostly bimodal in a composition containing sequences of alternating basalts, rhyolites, and trachytic lava flows. Tuff and ignimbrites are also common near the summit of these volcanoes (Kieffer et al., 2004).

2.3.3. Quaternary Volcanics

Quaternary volcanics in the northwestern Ethiopian plateau are exposed near the Tana graben. These volcanic products are alkaline basalts and trachytes which were erupted along with the preexisting structures. Volcanic cones and flows of scoriaceous basalts are well preserved in the Tana graben. Their relative unmodified geomorphological features such as the prevalence of prominent cinder cones and small collapse craters in a region of heavy rainfall and perennial streams indicate their recent age. From field, evidence suggested that these rocks are considered as Pleistocene in age (Mengesha Tefera et al., 1996; Adise Mekonnen, 2006).

Hofmann, (1997) noted that the host lavas are basanitic in composition and are dated 0.39 ± 0.03 Ma. According to Abbate et al., (1998) the basanites occur as massive, vesicular and fragmented rocks. They are aphyric to sparsely porphyritic containing phenocrysts abundant in olivine, plagioclase, clinopyroxene and occasionally nepheline set in a fine-grained matrix composed of the same phase as the phenocryst assemblage.

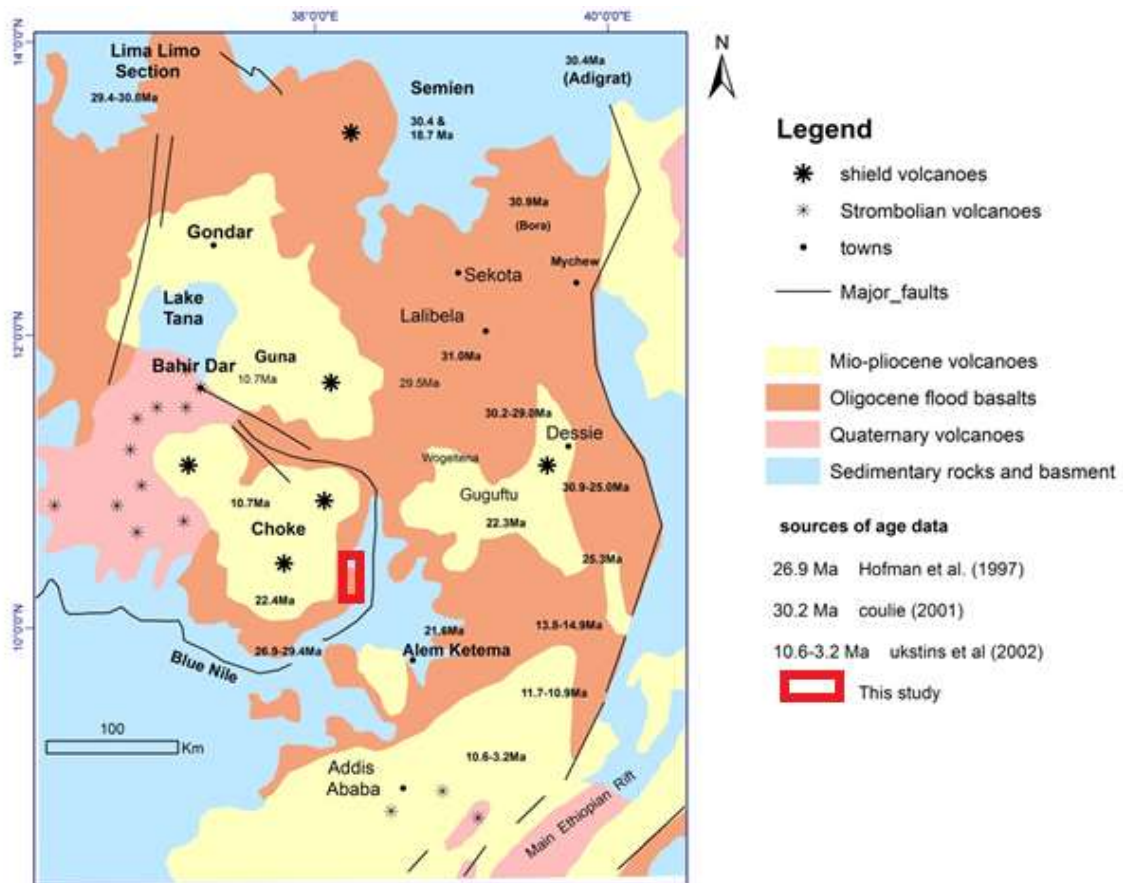


Figure.2.3. Regional geological sketch map of Ethiopia plateau (After Kieffer et al., 2004).

CHAPTER THREE

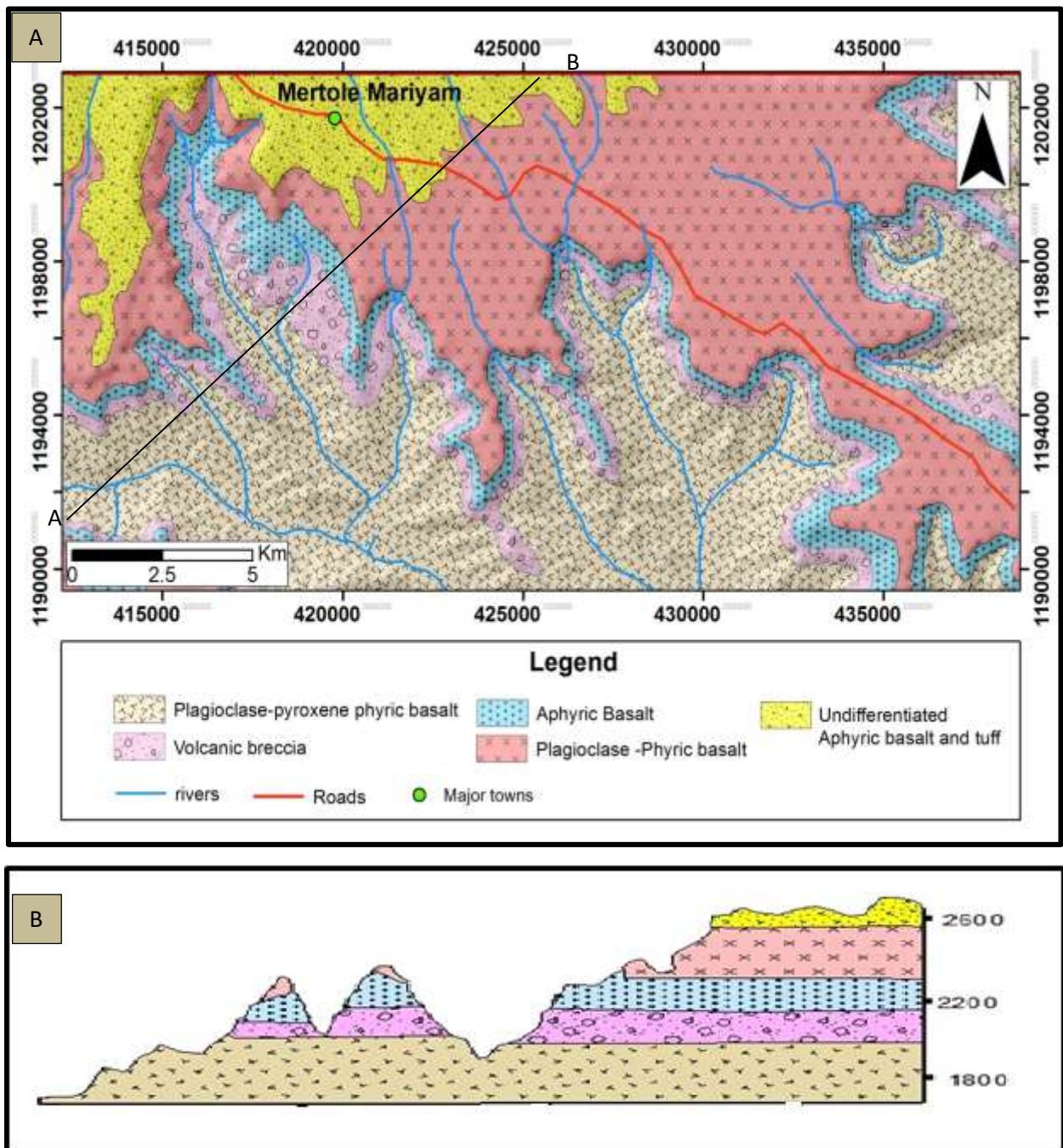
3. Geology of the study area

3.1. Introduction

The study area is located in the northwestern Ethiopian plateau in between Choke Miocene-Pliocene shield volcano and the Blue Nile Mesozoic sedimentary basin. The area is mostly covered with flood basalt volcanism. It is characterized by gentle slope around the town of Mertule Maryam and moderately to cliff forming in the south, east and west part of the town. The study mainly shows that the area comprises mafic lava of different field characteristics. The porphyritic basalts show dike intrusion encountered in the field. The distribution and volcanic succession of studied rock units are shown in the geological map of the study area. Hofmann et al. (1997) provided a $^{40}\text{Ar}/^{39}\text{Ar}$ age of 29.4-26.9 Ma on a sample taken from the Blue Nile river flood basalt.

3.2. Volcanic successions and petrographic descriptions

From the combination of studies in the field observation, petrographic investigation, geological mapping, and geochemical analysis; the Mertule Maryam locality volcanic products comprise plagioclase-pyroxene phyric basalt, volcanic breccia, aphyric basalt, and plagioclase phyric basalt and undifferentiated aphyric basalt interlayered with pyroclastic tuff. In addition, the plagioclase-pyroxene phyric basalt commonly intruded by basaltic dikes. Fresh and representative samples are utilized for petrographic and geochemical analysis. The field descriptions in outcrop scale, lithologic units with a geological map, geological cross-section, composite stratigraphic log section and petrographic description of the study area are presented in this chapter.



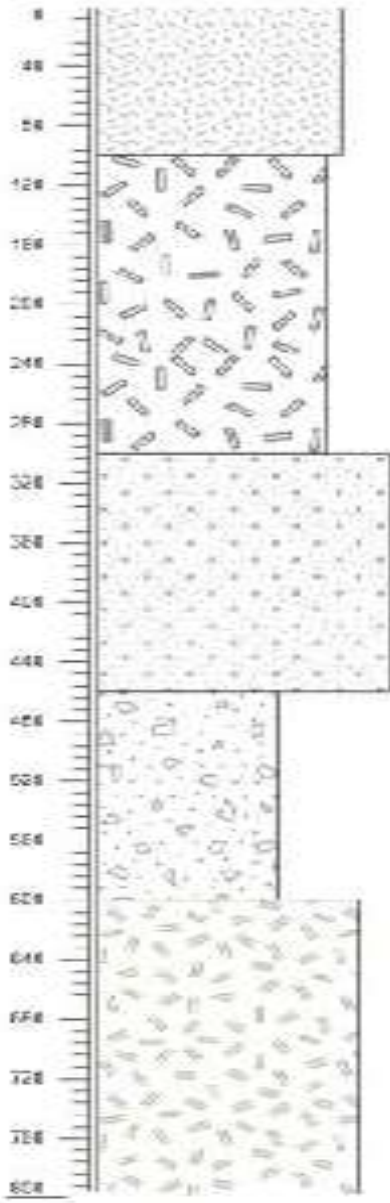
Stratigraphic Log	Description
	<p>Undifferentiated aphyric basalt and tuff (shows intercalation of tuff and columnar aphyric basalt)</p>
	<p>Plagioclase phyric basalt Porphyritic, massive, vesicular and shows columnar joint</p>
	<p>Aphyric basalt Cliff forming, sparsely porphyritic and shows columnar joint</p>
	<p>Volcanic breccia massive highly brecciated</p>
	<p>Plagioclase-pyroxene phyric basalt Porphyritic, massive, shows columnar joint intruded by dike</p>

Figure.3.2. Composite stratigraphic log section of Mertule Maryam area flood basalt volcanism.

3.2.1. Plagioclase-pyroxene phyric basalt

This rock unit is found relatively at a lower elevation, which is the lower basalt of the study area. It is mainly exposed in the southern, southwestern and southeastern part of Mertule Maryam town. This rock unit commonly forms moderately steep to gentle topographic features: - highly weathered and shows a range of colors from dark gray to yellowish- brown and reddish. The rock unit is characterized by dominant and large size phenocryst of plagioclase; which are visible from hand specimen scale and supported with a petrographic microscope. The rock unit is generally porphyritic with phenocrysts of plagioclase and pyroxene in which plagioclase is the dominant one and the groundmass is composed of fine-grained plagioclase laths, pyroxene and opaque minerals (e.g. Fe-Ti oxides). The rock unit shows amygdaloidal texture from field observation and porphyritic from petrographic investigation. This rock unit is commonly vesicular with subrounded to elliptical and elongated vesicles, partially filled by calcite, green zeolites, and rare quartz minerals. It is poorly exposed covered by farmland, showing layers of massive basalt, columnar jointed basalt and vesicular to scoriaceous basalts. Sample collected from this unit show alternate weathering and there is clearly identifiable feldspar which is colorless in physical observation. Representative samples were collected from this unit for petrographic and geochemical analysis.

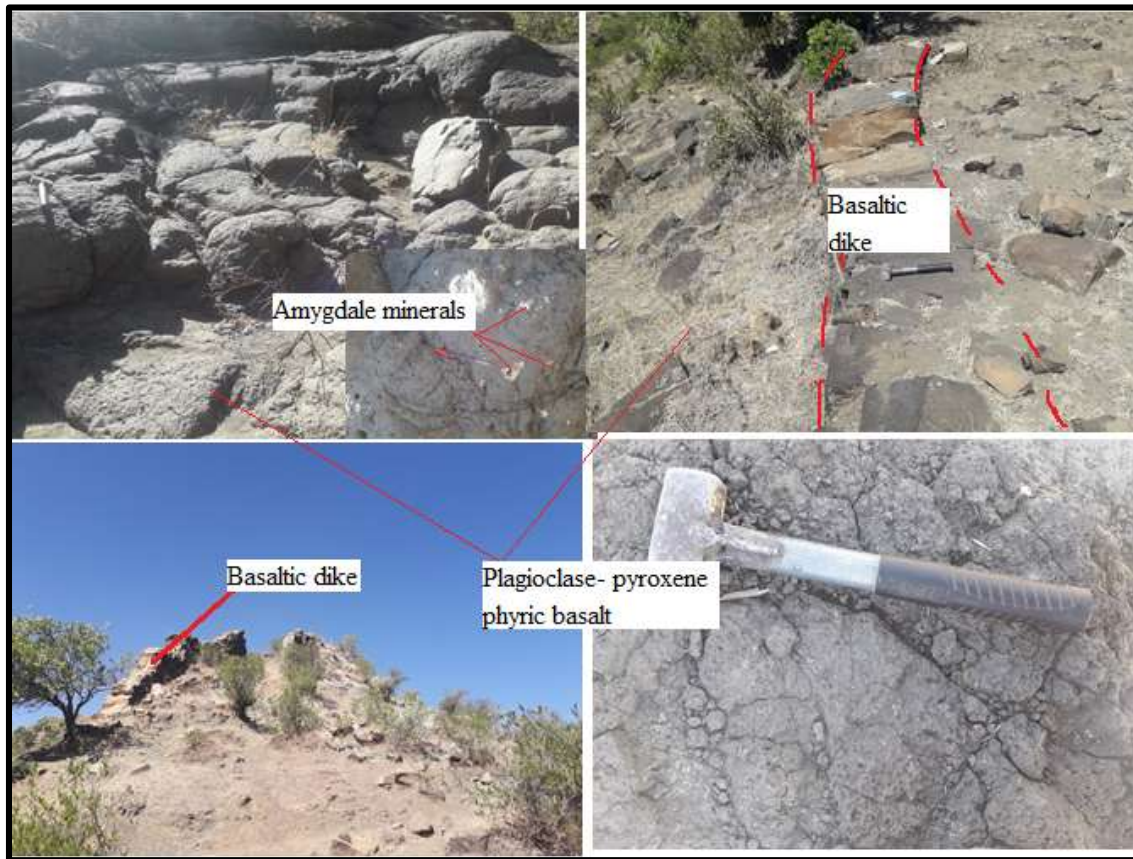


Figure.3.3. Close up views of porphyritic basalt from the southeastern and southwestern part of the plagioclase- pyroxene phyric basalt unit. The dike intrusions are also encountered in the porphyritic lower basalt unit.

Sample MS1S1 (Fig3.4 A) and sample MS4S1 (fig3.4 B) collected from southeastern and southwestern part from the lower flood basalt unit respectively. Petrographic investigation of the analyzed thin sections shows the dominant phenocryst is plagioclase. It shows polysynthetic twinning and zoning. The plagioclase phenocrysts show sieve texture and partly they are altered.

Sample MS1S1 is collected from the porphyritic basalt unit. Petrographic investigation shows the dominant phenocrysts are plagioclase and pyroxene with occasional olivine. The plagioclase phenocryst shows polysynthetic twinning and zoning. Sample MS1S1 is composed with modal percentage of 10 -15% phenocryst and 85-90% groundmass. The phenocryst assemblage shows plagioclase, pyroxene and olivine. These phenocrysts have subhedral to euhedral in shape with average grain size of 1- 4 mm. The groundmass is composed of fine-grained plagioclase lathes, interstitial pyroxene, olivine and opaque minerals (e.g.Fe-Ti oxide). The groundmass comprises of identifiable plagioclase laths, opaque and mafic

minerals. It is vesicular with subrounded to elongated vesicles field with calcite and green zeolites. In general, the thin section shows porphyritic texture comprises plagioclase and pyroxene phenocryst with microcrystalline groundmass.

Sample MS4S1 collected from the southwestern part of the study area from the porphyritic flow unit. Petrographic investigation shows the dominant phenocrysts are plagioclase and pyroxene. Plagioclase is the maximum phenocryst having euhedral shape and tabular form of texture with long direction size of ~ 6 mm, with pronounced polysynthetic twin, zoning, pikiolitic inclusion of mafic minerals, and alteration are common. Pyroxene phenocrysts have subhedral shape and it is partly altered. This sample shows pikiolitic inclusion of olivine and pyroxene enclosed with plagioclase.

Sample MS4S1 composed with a modal proportion of 20-25% phenocryst and 75-80% groundmass. The phenocrysts comprise plagioclase and pyroxene showing alteration. The groundmass is composed of plagioclase, opaque and mafic minerals. It shows porphyritic texture with plagioclase, pyroxene and microcrystalline groundmass.

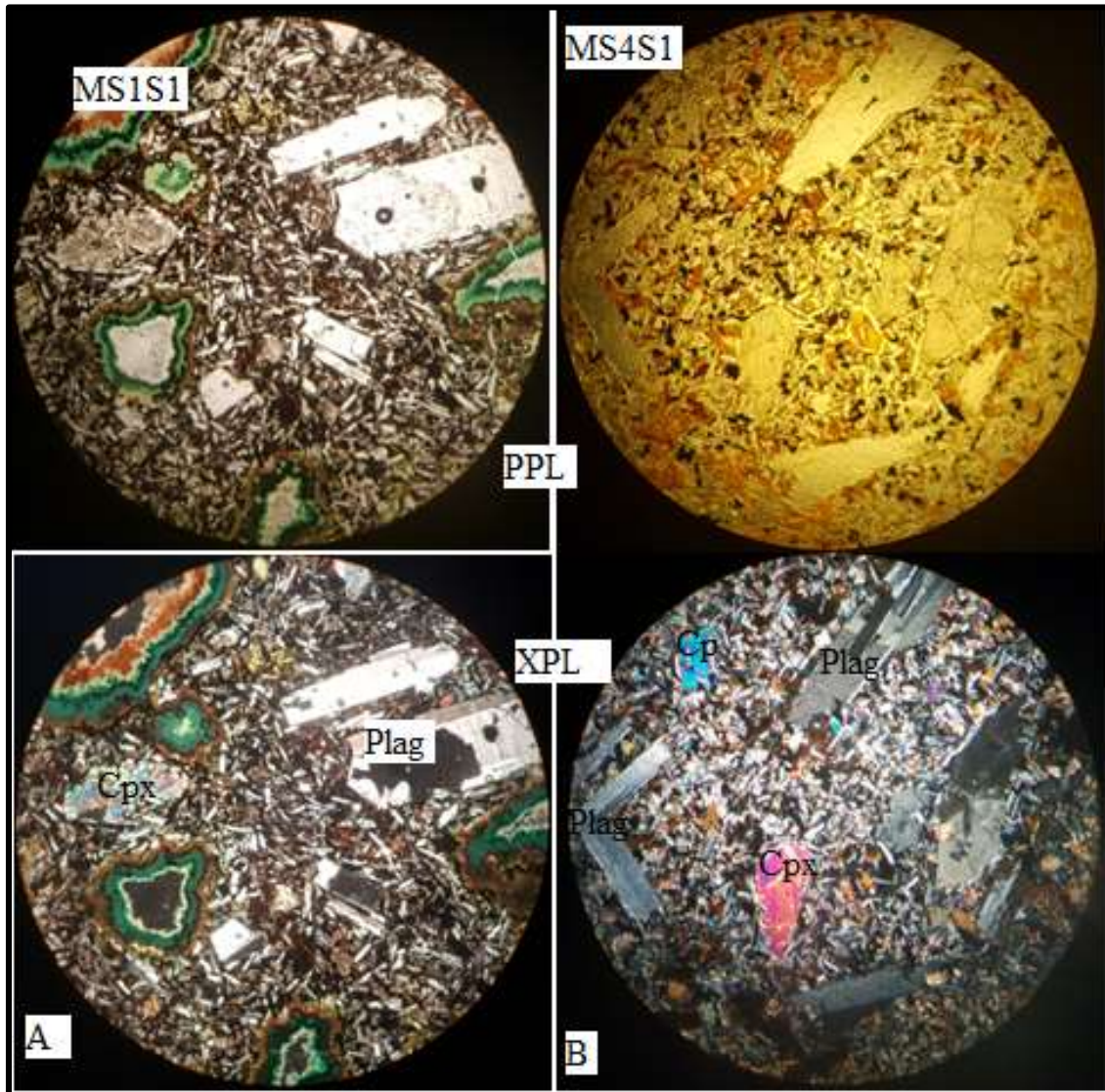


Figure.3.4. Microphotographs of plagioclase-pyroxene phyric basalt. Sample MS1S1 (A) showing plagioclase and pyroxene phenocrysts, the plagioclase phenocryst showing twinning and alteration; sample MS4S1 (B) showing plagioclase and pyroxene phenocrysts, plagioclase phenocryst showing polysynthetic twinning and zoning.

3.2.2. Agglomerate

This unit is found underlain by the porphyritic basalt unit and overlain by the aphyric basalt unit. It is generally brecciated that comprises crystals and rock fragments of different size. This unit contains clasts that are vesicular and some of the clasts are massive. The shape of the clasts is angular to subrounded. The amount and the size of the clasts increase from bottom to top of the unit. It forms moderately steep to gentle slope and shows a range of colors dark gray to reddish- brown for weathered part. It is usually massive and the vesicles of the clasts are filled with calcite. It is dominated with rock fragments comprising maximum

volcanic block size of about 40cm from field observation. The clasts are basaltic in composition and firm together by fine grained matrix. The unit is separated from the above aphyric basalt unit by paleosoil with a thickness of about 0.4 m.



Figure.3.5. close up views of agglomerate showing the nature of rock fragments and the shape of fragments with subrounded to angular fragments; also some of the rock fragments are massive whereas partly vesicular filled with calcite.

Sample MS1S2 (Fig3.6 A) and sample MS4S3 (Fig3.6 B) collected from the agglomerate unit respectively. Petrographic investigation of the analyzed thin sections dominated with rock fragments and occasional feldspar grains. The rest is covered with groundmass and calcite-filled in the voids of the rock fragments.

Sample MS1S2 collected from the agglomerate unit. From petrographic investigation the rock fragments are basaltic in composition. The agglomerate composed of 65% groundmass, 35% rock fragment, crystal of feldspar which shows sieve texture and calcite.

Sample MS4S3 collected from the agglomerate unit. From petrographic investigation of this thin section shows the modal percentages of 70% groundmass, 30% rock fragment and

calcite. The rock fragments found in this thin section are dominantly vesicular partly filled with calcite.

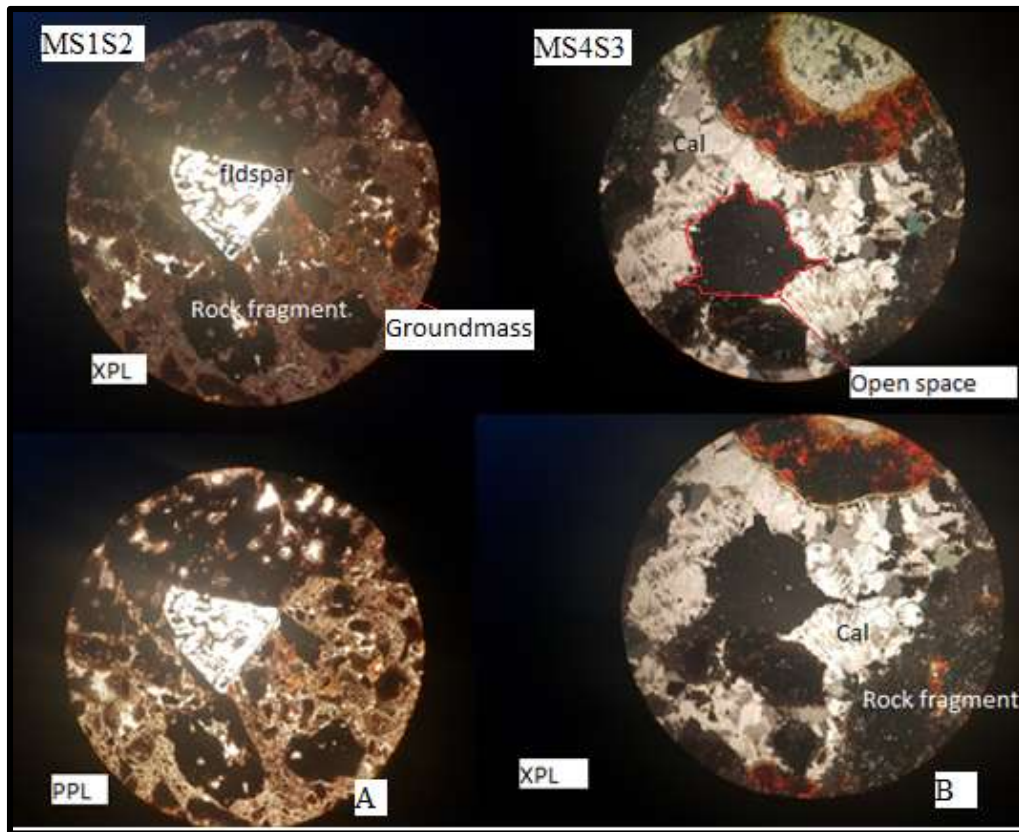


Figure.3.6. Microphotographs of volcanic breccia. Sample MS1S2 (A) showing occasional feldspar crystals and dominant rock fragments; sample MS4S3 (B) showing rock fragments and calcite-filled the vesicles of the rock fragments.

3.2.3. Aphyric basalt

This unit is found above the agglomerate unit and shows sharp topographic changes forming a sharp cliff above the moderately gentle agglomerate unit. This unit is commonly moderately steep to cliff forming topographic features and infrequently interlayered with pyroclastic tuff. It is generally aphyric with sparsely vesicular from field observation, weathered and shows a range of colors from dark black to brownish and yellowish. It is strongly fractured and highly columnar with sub-vertical to vertical joints. Moreover, these columnar basalts are sparsely vesicular and it has shining surface from field observation. The columns are also systematically arranged in some part of the outcrop. In addition to the aphyric columnar basalt sparsely porphyritic basalts are common in this unit. The interlayered pyroclastic tuff is

very fine-grained light gray to white, lightweight and slightly welded. It is massive and dominantly composed of ash-sized material.

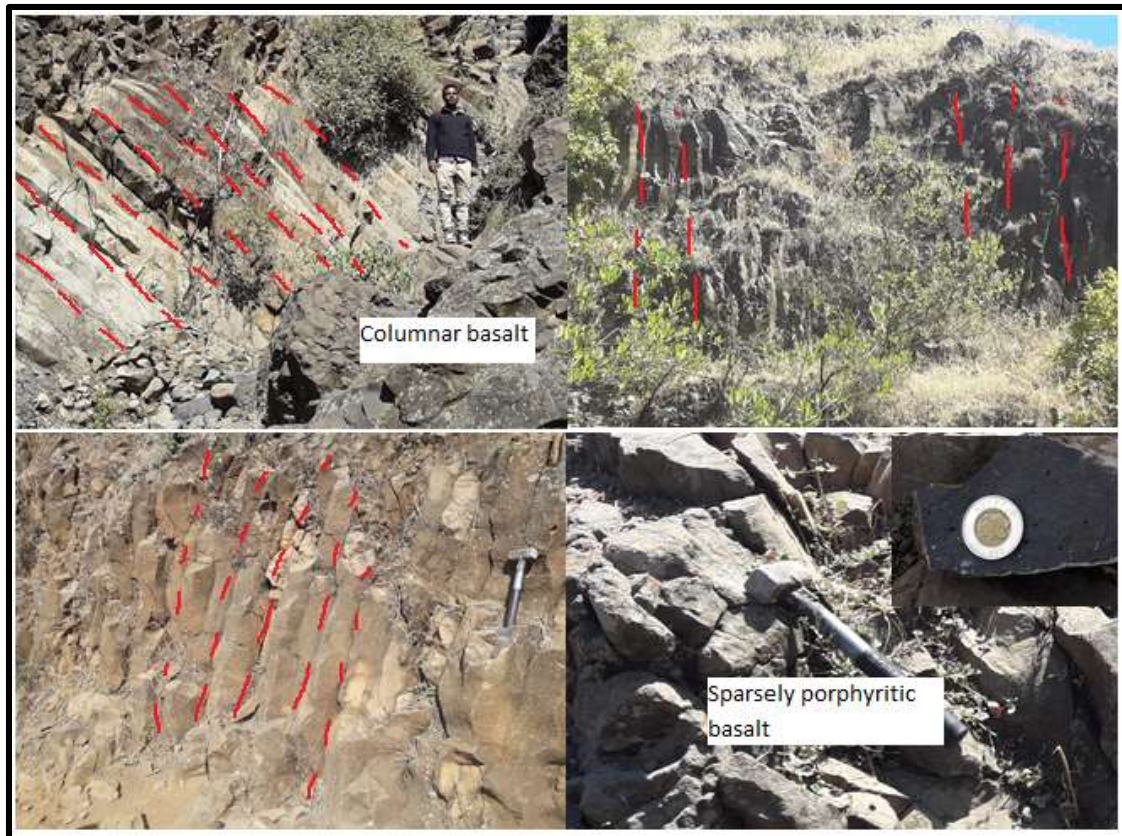


Figure.3.7. Close - up views of aphyric basalt which is cliff forming; strongly fractured and joined with vertical to sub-vertical joints, and columnar jointed with intercalation of sparsely porphyritic basalts.

Sample MS1S3 (Fig3.8 A), sample MS1S14 (Fig3.8 B) and sampleMS1S6 (C) collected from the aphyric basalt unit respectively. Petrographic investigation of the analyzed thin sections shows fine-grained identifiable plagioclase laths, opaque and indistinguishable fine-grained minerals.

Sample MS1S3 is collected from the aphyric basalt unit. It is composed of identifiable fine grained plagioclase, opaque and groundmass. The groundmass assemblage consists of fine grain materials with trachytic flow texture.

Sample MS1S4 collected from the aphyric basaltic unit from hand sample observation. It is aphyric and microcrystalline from petrographic observation. It is composed of identifiable

plagioclase minerals and groundmass. The groundmass is also composed of opaque and fine grained minerals with intergranular texture.

MS1S6 is collected from aphyric basaltic flow unit. It is aphyric in texture from hand specimen sample and microcrystalline in thin section. It is composed of 2- 3% phenocryst and 97-98% groundmass. The phenocryst assemblage is plagioclase with subhedral shape and commonly shows twinning. The groundmass is also composed of plagioclase laths, opaque and fine grained minerals. It has plagioclase glomerocrysts within microcrystalline groundmass texture. It is aphyric from hand specimen observation, whereas petrographic investigation shows poorly porphyritic.

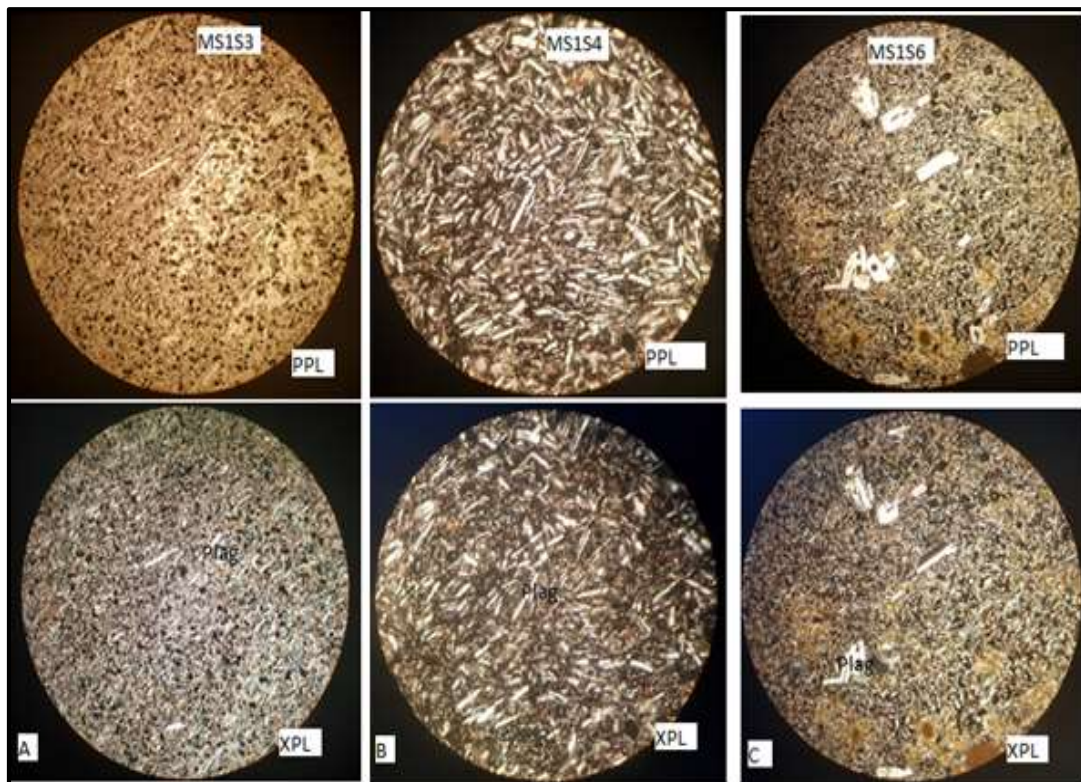


Figure.3.8. Microphotographs of aphyric basaltic flow unit. Sample MS1S3 (A) showing plagioclase laths and opaque with fine-grained groundmass; Sample MS1S4 (B) showing plagioclase laths in microcrystalline groundmass; sample MS1S6 (C) shows plagioclase phenocrysts in the microcrystalline groundmass.

Sample MS1S5 is collected from aphyric basalt flow unit which is sparsely vesicular basalt from hand specimen sample observation. Petrographic observation shows microcrystalline in

the thin section, with 10-15% opaque and 85-90% groundmass. The groundmass shows trachytic texture and composed of fine grained minerals.

Sample MS2S6 is collected from sparsely vesicular basalt unit, which is aphyric from hand sample observation. From petrographic observation, this thin section shows 1-2% plagioclase laths with 98-99% microcrystalline groundmass. The ground mass comprises of opaque and fine-grained minerals.

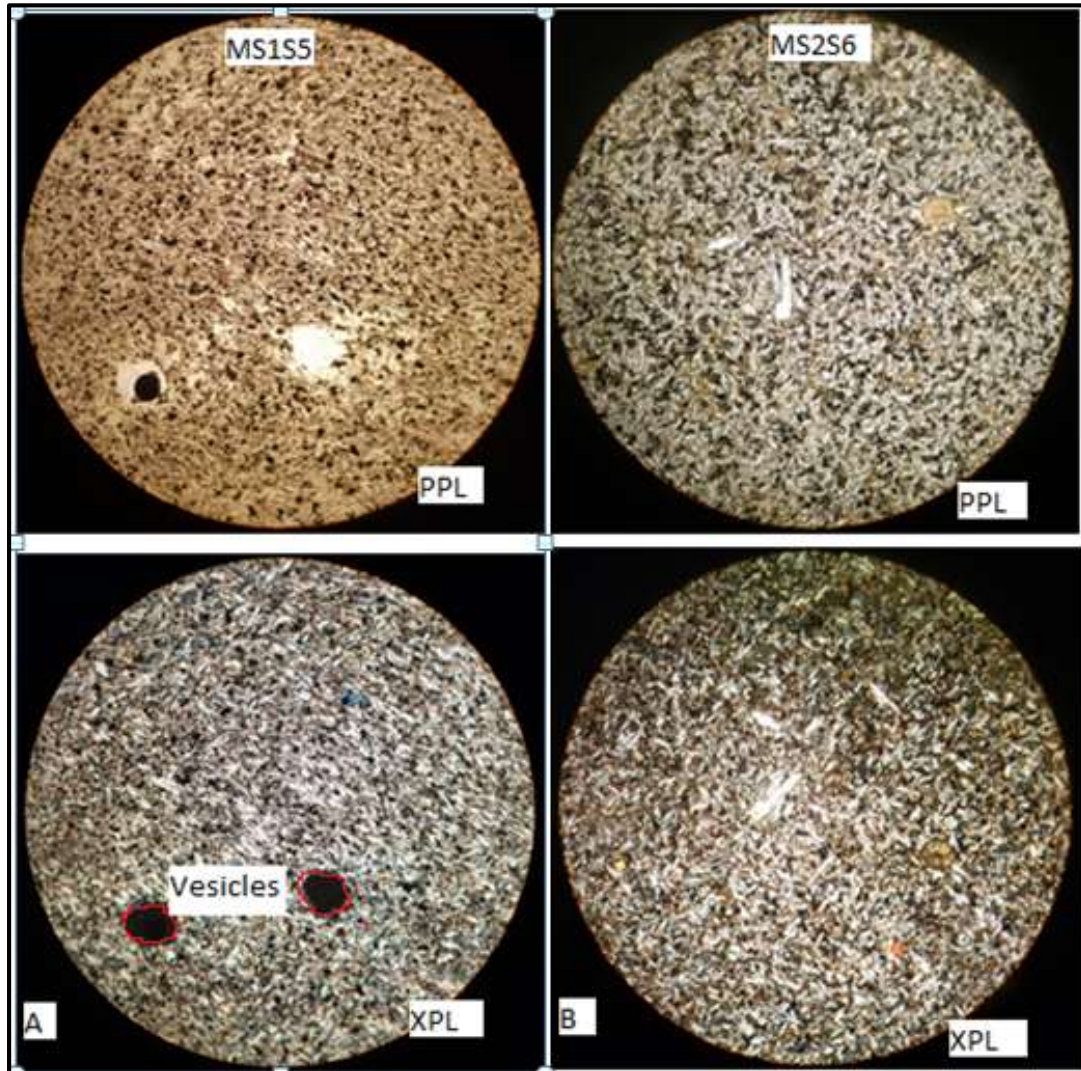


Figure.3.9. Microphotographs of aphyric basaltic flow unit. Sample MS1S5 (A) showing vesicles, plagioclase laths and opaque within fine-grained groundmass; Sample MS2S6 (B) shows plagioclase laths in the microcrystalline groundmass.

Sample MS2S1 collected from aphyric basalt unit showing columnar basaltic flow. It is aphyric in hand specimen sample and microcrystalline in thin section. Petrographic investigation shows few plagioclase laths with indistinguishable mineralogy in the

groundmass. The groundmass has textures vary as felty and trachytic. The thin section shows occasional plagioclase laths with anhedral shape. This Sample is composed of microcrystalline groundmass, which contains few plagioclase laths and dominant groundmass with opaque, mafic minerals.

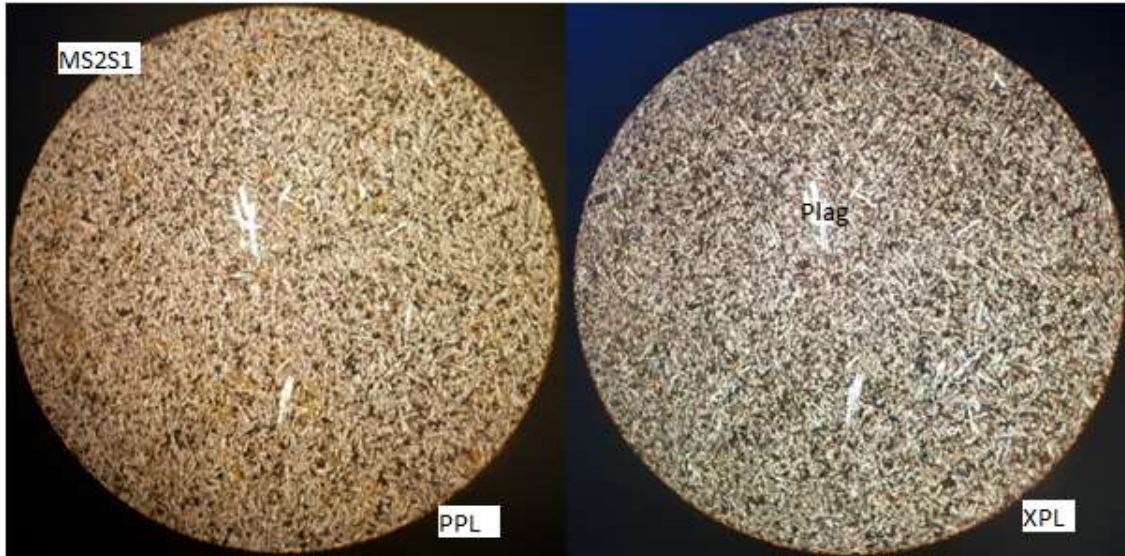


Figure.3.10. Microphotographs of aphyric basalt unit. Sample MS2S1 is taken from columnar lava flow shows plagioclase laths with fine-grained groundmass.

Sample MS2S3 collected from aphyric basalt unit; from the sparsely porphyritic lava flow. It is dark gray and sparsely porphyritic from hand sample observation. From petrographic observation plagioclase and olivine are dominant. It is composed of plagioclase, olivine grains and groundmass. The groundmass composed of opaque and fine-grained mafic minerals. The thin section shows intergranular texture discrete grains of mafic minerals filling the interstices of plagioclase laths.

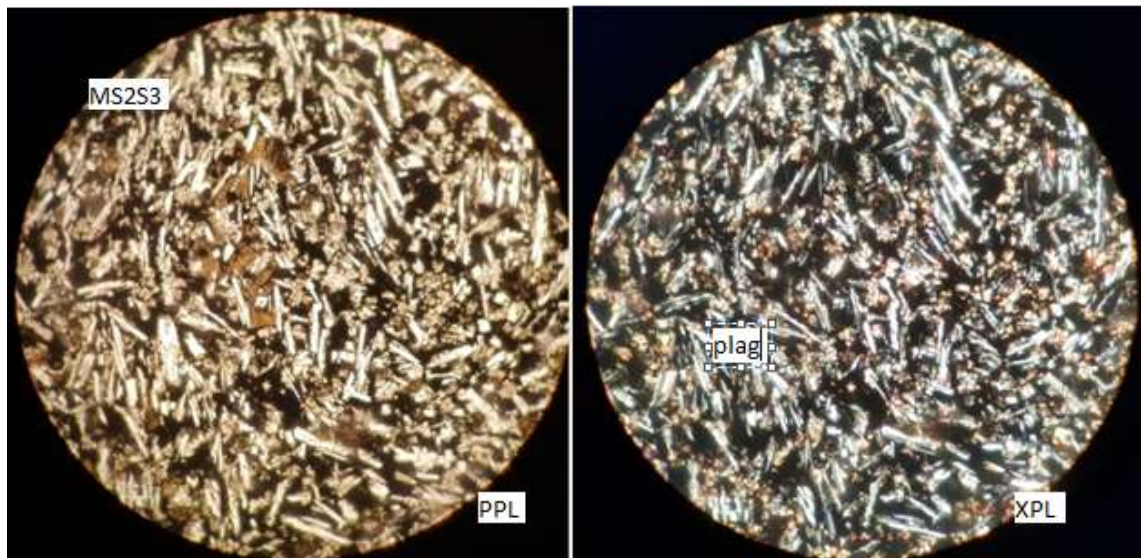


Figure.3.11. Microphotographs of aphyric basalt unit. Sample MS2S3 is taken from sparsely porphyritic lava flow shows plagioclase laths with fine-grained indistinguishable mafic minerals.

3.2.4. Plagioclase phyric basalt

This unit is extensively exposed in the southeastern part of the town of Mertule Maryam. It forms moderately gentle in topography and highly weathered. It comprises columnar, scoriaceous and porphyritic basalts interlayered with tuff at the upper part of the unit. It is highly weathered and shows dark gray, brownish to black color. The scoriaceous basalt is highly vesicular and massive. It is relatively lightweight and aphyric in texture from field observation. The columnar basalts are highly fractured disintegrated, showing aphyric texture from hand specimen sample observation. The columnar basalts are sparsely vesicular and showing sub-vertical to vertical joints. The porphyritic basalt is characterized by dominant and large size phenocrysts of plagioclase which are visible from hand specimen scale and supported with a petrographic microscope. It is poorly exposed, covered by grass and farmland showing massive structure. This rock unit is highly affected by spheroidal weathering at the upper part of the unit.

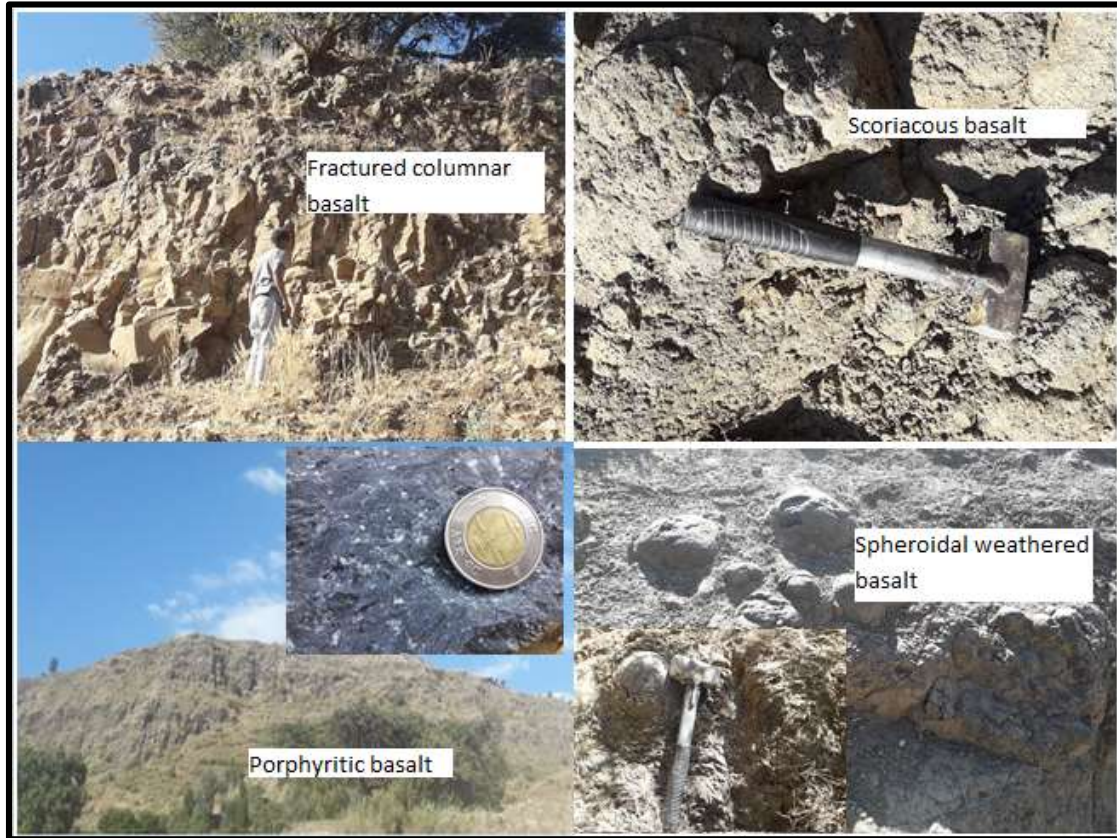


Figure.3.12. close-up views of plagioclase phyric basalt unit showing highly fractured columnar basalt, scoriaceous basalt, porphyritic basalt, and spheroidal weathered basalt.

Sample MS2S9 is collected from the plagioclase phyric basalt unit with columnar lava flow showing aphyric texture in hand specimen sample and sparsely porphyritic in thin section. Petrographic observation of this rock unit shows 2-3% phenocrysts of plagioclase and 97-98% of the groundmass. The texture of this sample is glomerocryst clots of plagioclase grains in the microcrystalline groundmass. The groundmass composed of plagioclase (feldspar), mafic minerals and other minerals.

Sample MS2S10 collected from the plagioclase phyric basalt unit with columnar lava flow. It is aphyric texture in hand specimen sample observation supported with the petrographic investigation. Petrographic investigation of this sample shows plagioclase laths, opaque and fine grained groundmass.

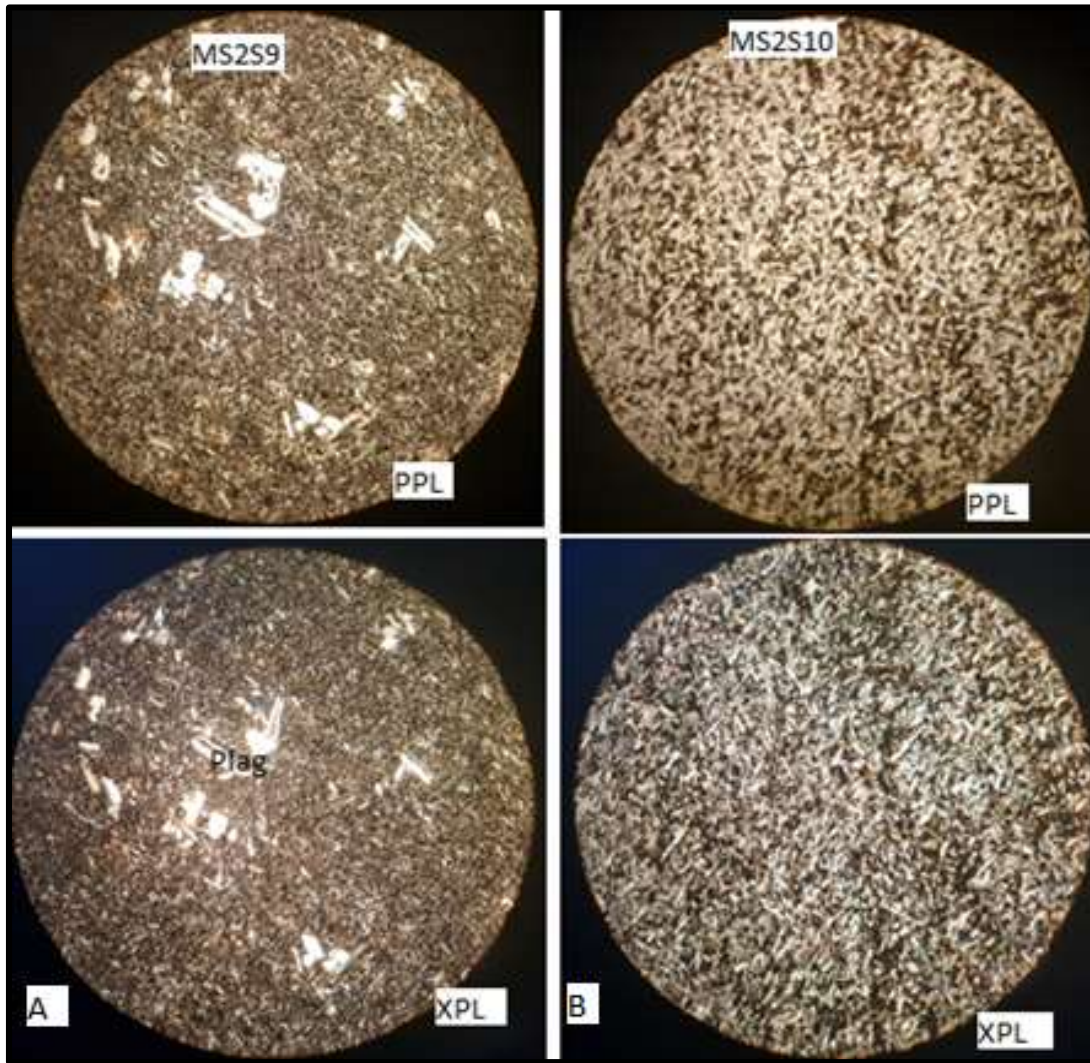


Figure.3.13. Microphotographs of columnar lava flow unit; Sample MS2S9 (A) showing plagioclase phenocrysts with fine-grained indistinguishable minerals; sample MS2S10 (B) showing identifiable plagioclase laths and groundmass.

Sample MS3S2 collected from the plagioclase phyric basalt unit. It is sparsely porphyritic from hand specimen observation. Petrographic investigation shows this sample composed of plagioclase laths, mafic minerals, and groundmass. The groundmass comprises of opaque and fine-grained minerals with sub ophitic texture.

Sample MS3S4 collected at 2,374 m above mean sea level from the sparsely porphyritic lava flow. It is dark black and sparsely porphyritic from hand specimen sample observation. Petrographic analysis of this thin section shows plagioclase, pyroxene, opaque and groundmass with intergranular texture of groundmass. The indistinguishable mafic minerals are enclosed by plagioclase laths.

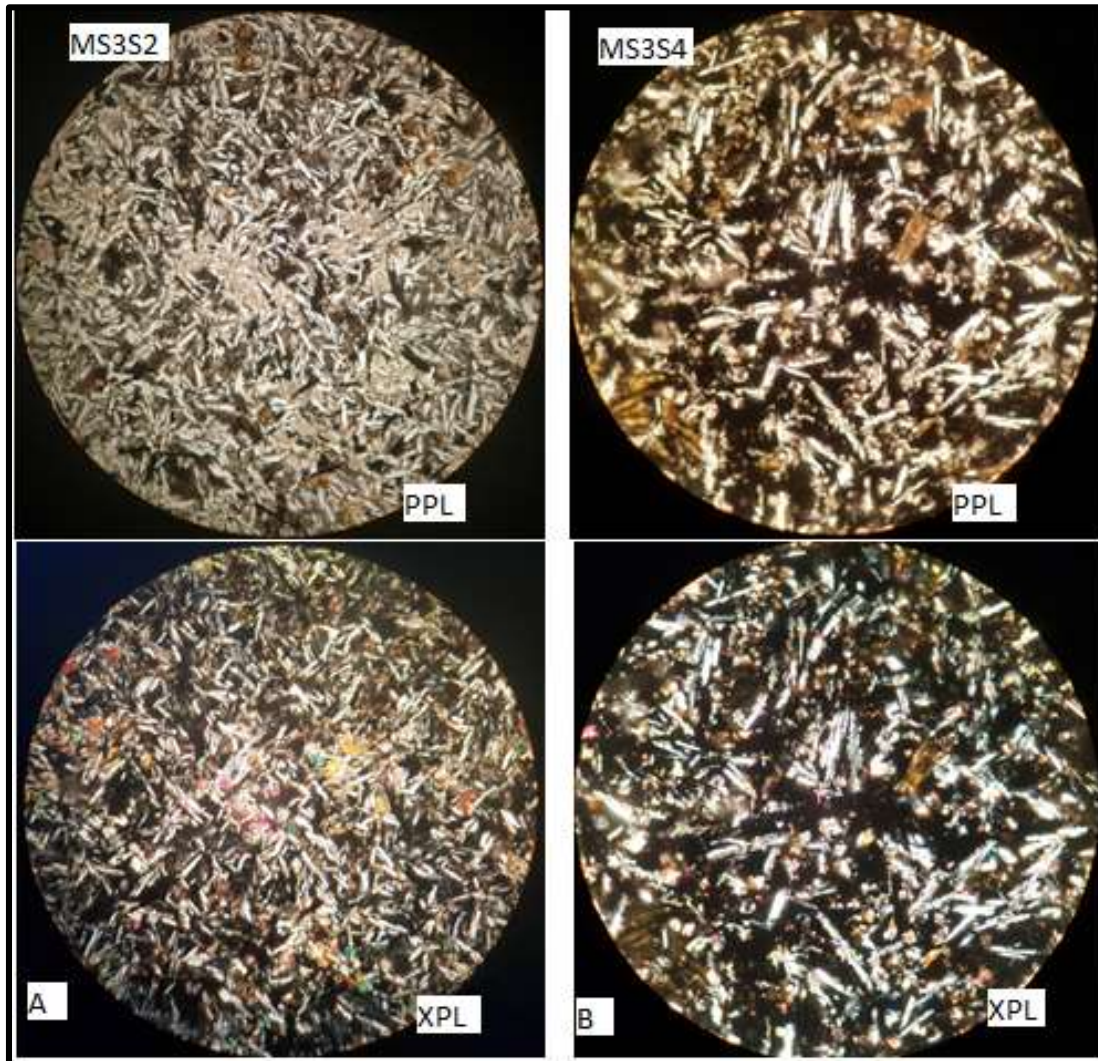


Figure 3.14. Microphotographs of sparsely porphyritic lava flow units; Sample MS3S2 (A) showing identifiable olivine and plagioclase laths with fine-grained indistinguishable minerals; sample MS3S4 (B) showing identifiable pyroxene and plagioclase laths and indistinguishable mafic minerals.

Sample MS5S1 (Fig3.15 A) and sample MS5S2 (fig3.15 B) collected from the plagioclase phytic basalt near the town of Mertule Maryam respectively. Petrographic investigation of the analyzed thin sections shows the dominant phenocryst phase is plagioclase. It shows characteristic features of pronounced polysynthetic twinning and zoning. It shows pikiolitic inclusion of pyroxene enclosed by plagioclase.

Sample MS5S1 composed with a modal percentage of 30-35% phenocryst and 65-70% groundmass. The groundmass assemblage comprises plagioclase, pyroxene, olivine and opaque minerals.

Sample MS5S2 composed with modal percentage of 10-15% phenocryst and 85-90% groundmass. The groundmass comprises of fine grained mafic minerals, opaque and other accessory minerals.

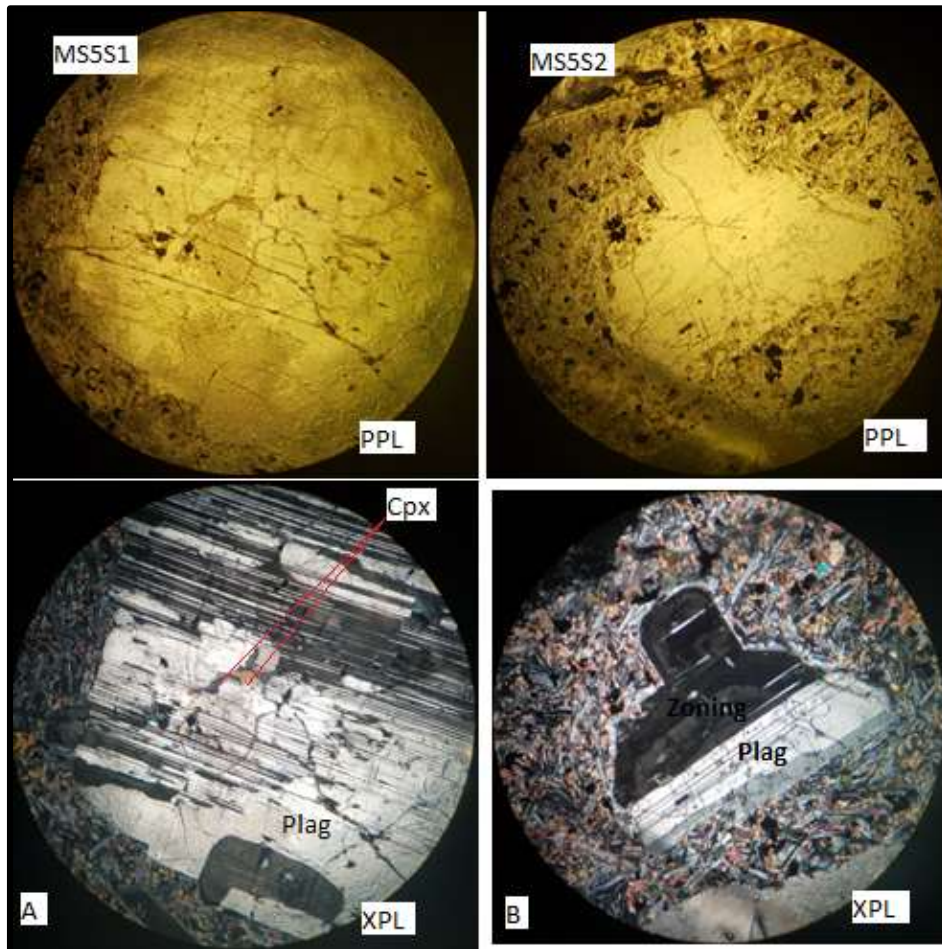


Figure.3.15. Microphotographs of plagioclase phenocrysts in basalt. Sample MS5S1 (A) showing polysynthetic twinning and poikilitic inclusion of pyroxene in tabular plagioclase; sample MS5S1 (B) showing plagioclase feldspar grains forming multiple twins and zoning.

3.2.5. Undifferentiated aphyric basalt and tuff

This unit is exposed in the northwestern and northern part of the study area around the town of Mertule Maryam, forming hills, moderately slope to flat - laying topography. It is columnar jointed with vertical to sub-vertical joints; intercalated with pyroclastic tuff. The basalt flows are aphyric from hand specimen sample observation confirmed with a petrographic investigation of fresh samples of columnar basalt lava flow unit. It is highly

weathered showing a range of colors from dark gray to black and brown. The pyroclastic tuff is dominantly white, fine-grained, lightweight and interlayered with the aphyric basalt. Occasionally, it is thinly bedded/laminated; highly weathered and friable showing a range of colors like white, light gray to brown from field observation. It is poorly exposed, covered by farmland and grass, showing massive structure.



Figure.3.16. Close-up views of weathered aphyric columnar basalt interlayered with thinly bedded and massive pyroclastic tuff.

Sample MS5S3 (Fig3.17 A) and sample MS5S4 (fig3.17 B) collected from the aphyric columnar basalt unit northeastern and northwestern part of the town of Mertule Maryam respectively. Petrographic investigation of the analyzed thin sections shows the sample is composed of plagioclase laths and trachytic texture groundmass.

Sample MS5S3 composed of a modal percentage of 1-3% phenocryst and 97-99% groundmass. The groundmass comprises plagioclase, opaque and other minerals.

Sample MS5S4 collected from the aphyric columnar lava flow unit composed of identifiable plagioclase laths and groundmass that shows trachytic flow texture.

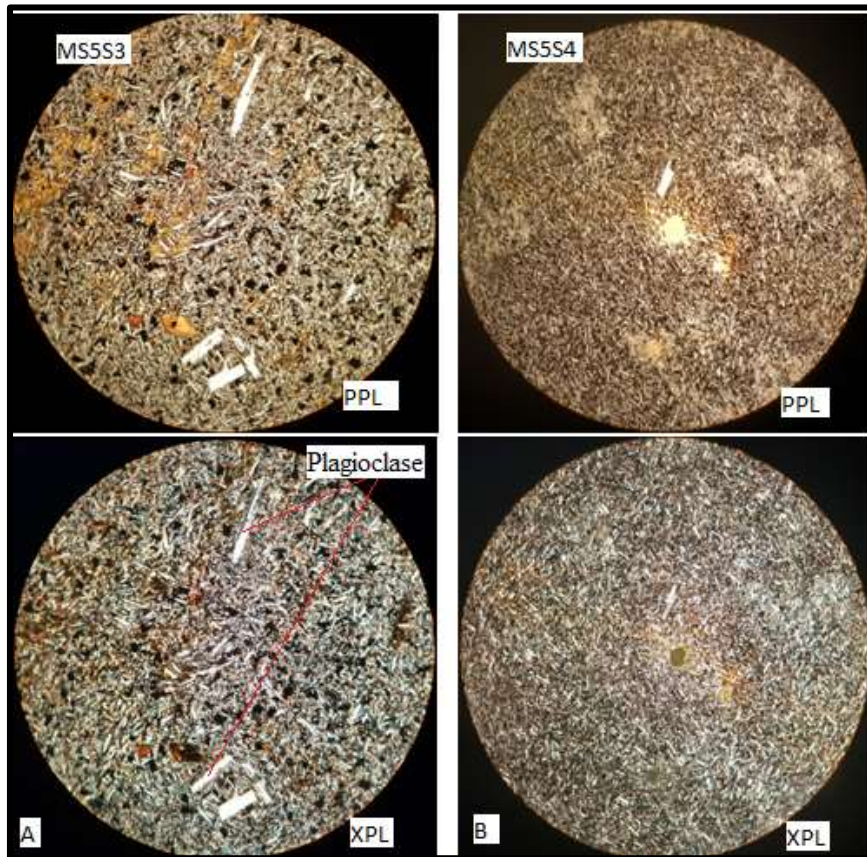


Figure.3.17. Microphotographs of aphyric basalt taken from the columnar lava flow; sample MS5S3 (A) showing plagioclase phenocrysts in trachytic groundmass; sample MS5S4 (B) showing few identifiable plagioclases in the fine-grained groundmass.

3.2.6. Basaltic dike

In the southwestern part of the study area near the contact between the plagioclase-pyroxene aphyric basalt and volcanic breccia unit there is dike intrusion (see fig 3.3). The dike intrudes the porphyritic basalt unit showing aphyric texture at hand specimen scale. Petrographic study shows the sample is not fully aphyric (2-3% pyroxene phenocryst) and 97-98% groundmass. The groundmass comprises opaque and other mafic minerals.

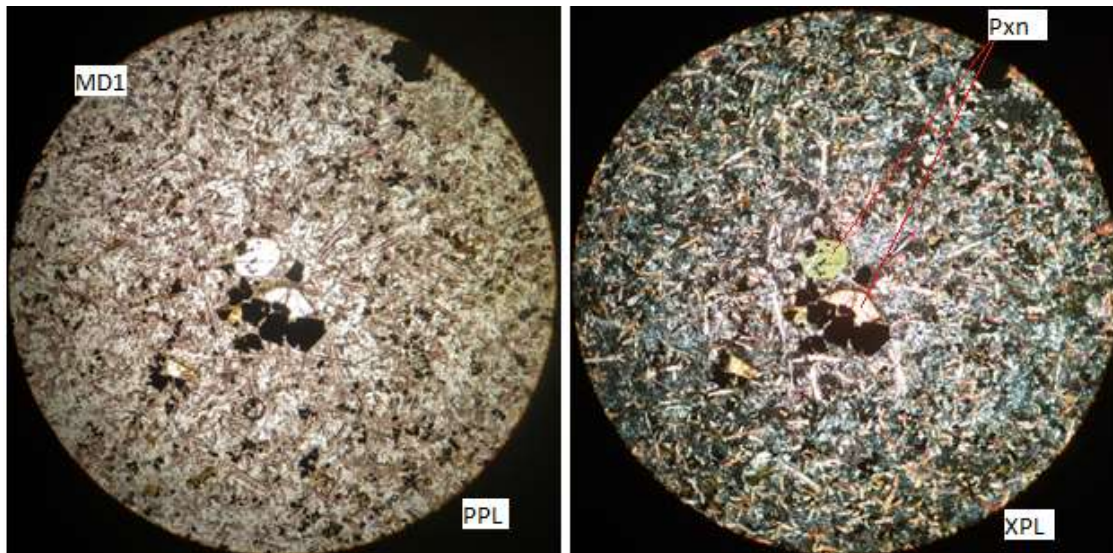


Figure.3.18. Microphotograph of a basaltic dike. Sample MD1 taken from basaltic intrusion with aphyric microcrystalline texture, viewed at 4X magnification.

CHAPTER FOUR

4. Whole rock geochemistry

4.1. Introduction

To understand the magmatic evolution and geological process experienced in any volcanic product geochemistry is an essential tool in studying the chemical signature of a rock. To achieve the study a total of seven fresh samples were selected for whole rock geochemical analysis. The selected samples were submitted to the Australian Laboratory service (ALS) for major element, trace, and rare earth elements analysis.

Major element, trace element, and volatile geochemical data types are identified from this study. Major and trace element data types are used to understand the evolution of the volcanic products in the study area. Whereas, volatiles are used to determine alteration effects of analyzed samples presented by Loss on Ignition (LOI); LOI represents the total volatile content of the rock that is generated by igniting the analyzed rock sample with temperature of 1000°C. The value of LOI in these samples ranges from 0.56(MS3S5) to 3.75 (MS5S4).

Analytical data for major oxides, trace, and rare earth element data including CIPW norms and LOI for the analyzed samples are presented in table 4.1. Numerous variation diagrams for major element oxides versus silica, trace element versus silica, trace element versus trace element constructed. Chondritic normalized rare earth elements (REE) abundance patterns and primitive mantle normalized incompatible trace elements patterns in multi-element spider diagrams are plotted for the analyzed samples.

Table 4.1. Geochemical data of Mertule Maryam area volcanics presented as major oxide and LOI (wt %) and trace element data (ppm) and CIPW normative mineral data (wt %) respectively.

Field code	MS1S5	MS1S3	MS5S3	MS5S4	MS2S9	MS2S10	MS4S1
rock name							
SiO ₂	51	50.1	50.5	47.7	49.7	50	48.5
TiO ₂	3.13	3.17	3.11	2.63	3.12	2.96	3.3
Al ₂ O ₃	13.4	13.75	13.65	13.45	13.55	13.4	13.9
FeO ₃	13.75	13.95	14.55	13.85	15.15	15.4	14.7
MgO	4.17	4.68	4.64	4.7	4.82	4.7	4.76
MnO	0.27	0.2	0.21	0.19	0.2	0.21	0.17
CaO	7.83	8.81	8.66	9.73	9.15	8.59	9.16
Na ₂ O	3.32	2.87	2.73	2.44	2.79	2.79	2.63
K ₂ O	0.58	0.51	0.89	0.5	0.58	0.79	0.5
P ₂ O ₅	1.09	0.46	0.45	0.3	0.42	0.39	0.33
LOI	0.61	1.56	0.56	3.75	1.1	1.22	1.97
Total	99.15	100.06	99.95	99.24	100.58	100.45	99.92
CIPW Normative minerals for analyzed samples (wt %)							
Quartz	7.6363	6.2433	6.1019	4.5412	5.0132	5.2413	4.9153
Anorthite	18.641	21.822	21.056	22.964	21.429	20.4	23.339
Diopside	10.672	15.343	15.46	19.036	17.309	16.086	16.23
Hypersthene	11.867	10.854	11.289	9.8671	11.29	12.064	10.972
Albite	28.093	24.285	23.1	20.647	23.608	23.608	22.254
Orthoclase	6.0415	5.6279	7.8735	5.5688	6.0415	7.2826	5.5688
Apatite	2.5255	1.0658	1.0426	0.6951	0.9731	0.9036	0.7646
Ilmenite	5.9446	6.0205	5.9066	4.9949	5.9256	5.6217	6.2674

Magnetite	19.936	20.226	21.096	20.081	21.966	22.329	21.314
Sum (wt %)	111.36	111.49	112.93	108.39	113.55	113.54	111.62
Li	<10	10	10	10	10	10	10
Sc	23	25	25	28	26	27	23
V	191	380	377	373	425	424	376
Cr	10	10	10	50	20	20	150
Co	17	40	43	40	45	36	41
Ni	9	16	17	54	24	31	94
Cu	21	25	23	94	28	85	201
Zn	166	148	141	124	137	138	137
Ga	26.3	23.7	23.8	21.5	22.6	23.9	26.5
As	<5	<5	<5	<5	<5	<5	<5
Rb	9.1	10	15.5	10.2	10.7	14	10.5
Sr	553	450	463	389	451	389	394
Y	51.4	32.6	33.4	29	29.8	35.1	38.8
Zr	255	217	224	161	196	198	248
Nb	27.8	20.3	19.7	13.3	18.1	15.8	20.6
Mo	1	1	2	<1	1	1	2
Ag	<0.5	<0.5	<0.5	<0.5	<0.5	<0.5	0.5
Cd	<0.5	<0.5	<0.5	<0.5	<0.5	0.8	<0.5
Sn	2	2	2	2	2	2	2
Cs	0.19	0.25	0.28	0.16	0.26	0.16	0.27
Ba	217	232	193	149	162.5	252	160
La	30.6	21.1	21.1	14.9	19.1	19.1	21.9
Hf	6.6	5.8	5.8	4.3	5.5	5.5	6.7

Ta	2.7	1.5	2	1.3	1.4	1.2	1.5
W	1	1	1	2	1	1	2
Ti	<10	<10	<10	<10	<10	<10	10
Pb	9	9	5	5	4	6	13
Ce	73.3	48.9	48.9	35	44.7	43.6	51.4
Pr	10.75	6.92	6.93	5.08	6.37	6.54	7.27
Nd	49.2	30.9	30.5	22.9	28.4	28.3	32.3
Sm	13	7.84	7.81	6.45	7.47	7.5	8.73
Eu	4.95	2.68	2.62	2.11	2.48	2.51	2.76
Gd	14.5	8.46	8.41	7.04	7.96	8.15	9.42
Tb	2.01	1.23	1.23	1.1	1.16	1.23	1.39
Dy	10.8	6.79	6.95	5.71	6.65	7.13	7.74
Ho	2	1.28	1.33	1.11	1.24	1.34	1.49
Er	5.07	3.28	3.4	2.95	3.09	3.57	3.7
Tm	0.68	0.44	0.45	0.39	0.44	0.47	0.49
Yb	3.7	2.6	2.58	2.2	2.61	2.95	2.83
Lu	0.51	0.37	0.39	0.34	0.37	0.44	0.4
Th	2.37	2.14	2.14	1.18	2.02	1.57	2.22
U	0.82	0.7	0.72	0.41	0.69	0.5	0.71

4.2. Chemical variation diagrams

4.2.1. Classification variation diagram

For the success of this study two variation diagrams have been used which are major and trace element. Based on silica content (SiO_2 %) igneous rocks are classified into, felsic >66 wt%, intermediate 52-66 wt%, mafic 45 to 52 wt% and ultra-mafic <45 wt%. Based on this classification the analyzed samples from Mertule Maryam area volcanic products are fall in the mafic range (47.7-51). Major element variation diagram of SiO_2 versus $\text{Na}_2\text{O} + \text{K}_2\text{O}$ (wt %) used to classify rock suites based on chemical composition. Based on Total alkali-silica (TAS) classification diagram (after Le Bas et al, 1986) the analyzed rocks are classified as basalts.

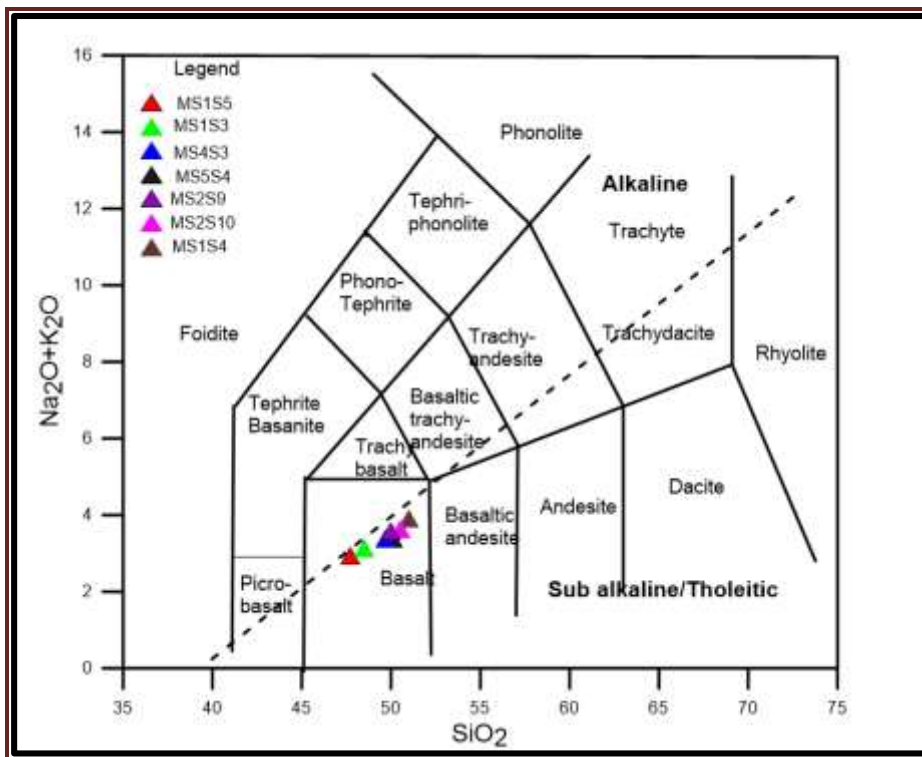


Figure.4.1. Total alkali-silica (TAS) classification diagram after Le Bas et al., (1986) for analyzed samples, Mertule Maryam volcanic areas.

4.2.2. Major element variation diagram

The geochemical data of the basaltic samples presented above in table form is also displayed below in diagram form as binary and normalized (spider and REE pattern). The purpose of utilizing variation diagrams is to characterize the analyzed rock samples of the study area and to interpret chemical differences and trends of the analyzed rocks. The Mg# is taken as the x-axis and used as differentiation index in variation diagrams constructed for major element oxides. Major element concentration is variable for the analyzed rock samples. These samples constitute 47.7-51% SiO₂, 13.4-13.9% Al₂O₃, 13.75 -15.4% Fe₂O₃, 4.17 – 4.82% MgO, 7.83 – 9.73% CaO, 2.44 – 3.32% Na₂O, 0.5 – 0.89% K₂O, 2.63-3.3% TiO₂ and, 0.3-1.09% P₂O₅. Alteration and weathering rate of analyzed rocks are determined from loss on ignition (LOI). This result shows the percentage of LOI from 0.56 to 3.75 (wt %), which indicates that these rocks are subjected to a different degree of alteration and weathering processes. Sample MS5S4 showing LOI percent of 3.75 (wt %) confirming more alteration effects observed during field investigation. The remaining samples show LOI percent of <2 (wt %) showing less effect of alteration and weathering. From the diagram is shown below strong scattered correlation of basaltic samples is presented in Mg# versus SiO₂, TiO₂, Fe₂O₃, Na₂O₃ and the remaining major oxides which is not shown. The Mg# is calculated by the formula

$$\text{Mg\#} = (\text{Mg}/\text{Mg}+\text{Fe}^{2+}) * 100.$$

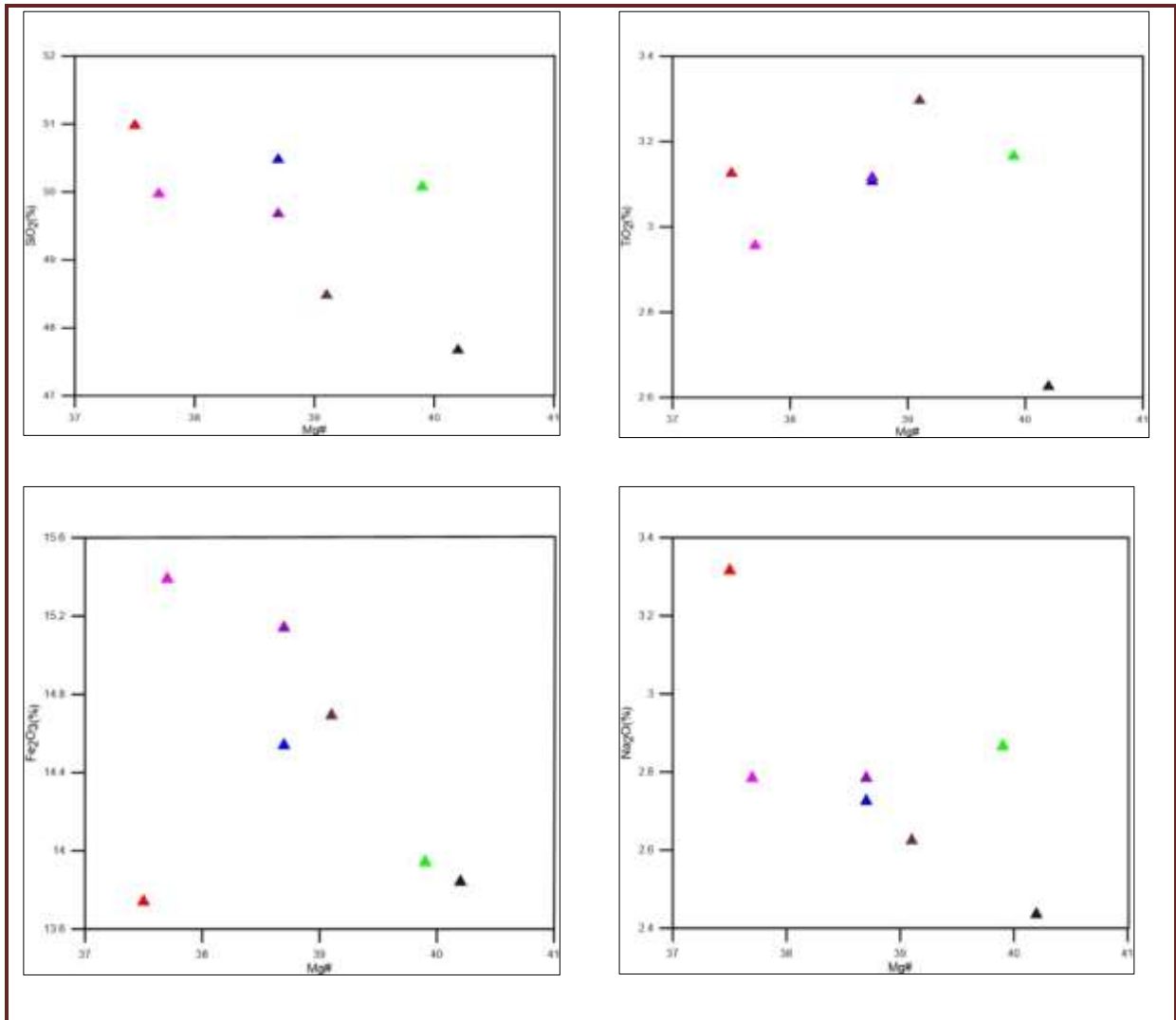


Figure.4.2. Variation diagrams of selected major element abundances (wt %) as a function of Mg# content for analyzed samples, Mertule Maryam volcanic area (see legend fig 4.1).

4.2.3. Trace element variation diagram

Trace element is small fractions of phases with concentration <0.1 (wt %) expressed in (ppm). These elements are the second group of geochemical data analyzed, synthesized and presented in this chapter. In addition to the major oxide data, the trace elements give geochemical and geological information. Trace elements can be grouped in to compatible and incompatible due to their preference into the solid or to the melt. To understand the geological process takes place during the formation of Mertule Maryam area volcanic products the following incompatible trace elements are going to be used. The Low field

strength (LFS) elements (i.e. Sr, Eu, and Ba) and high field strength (HFS) elements (e.i. Zr, La, U, Th, Hf, Ta and Nb).

Variation diagrams for incompatible element concentration (ppm) as functions of magnesium are plotted in fig 4.3; shows scattered correlation trends. Variation diagram in Sr, Eu, and Ba generally shows scattered trend as a function of Mg#.

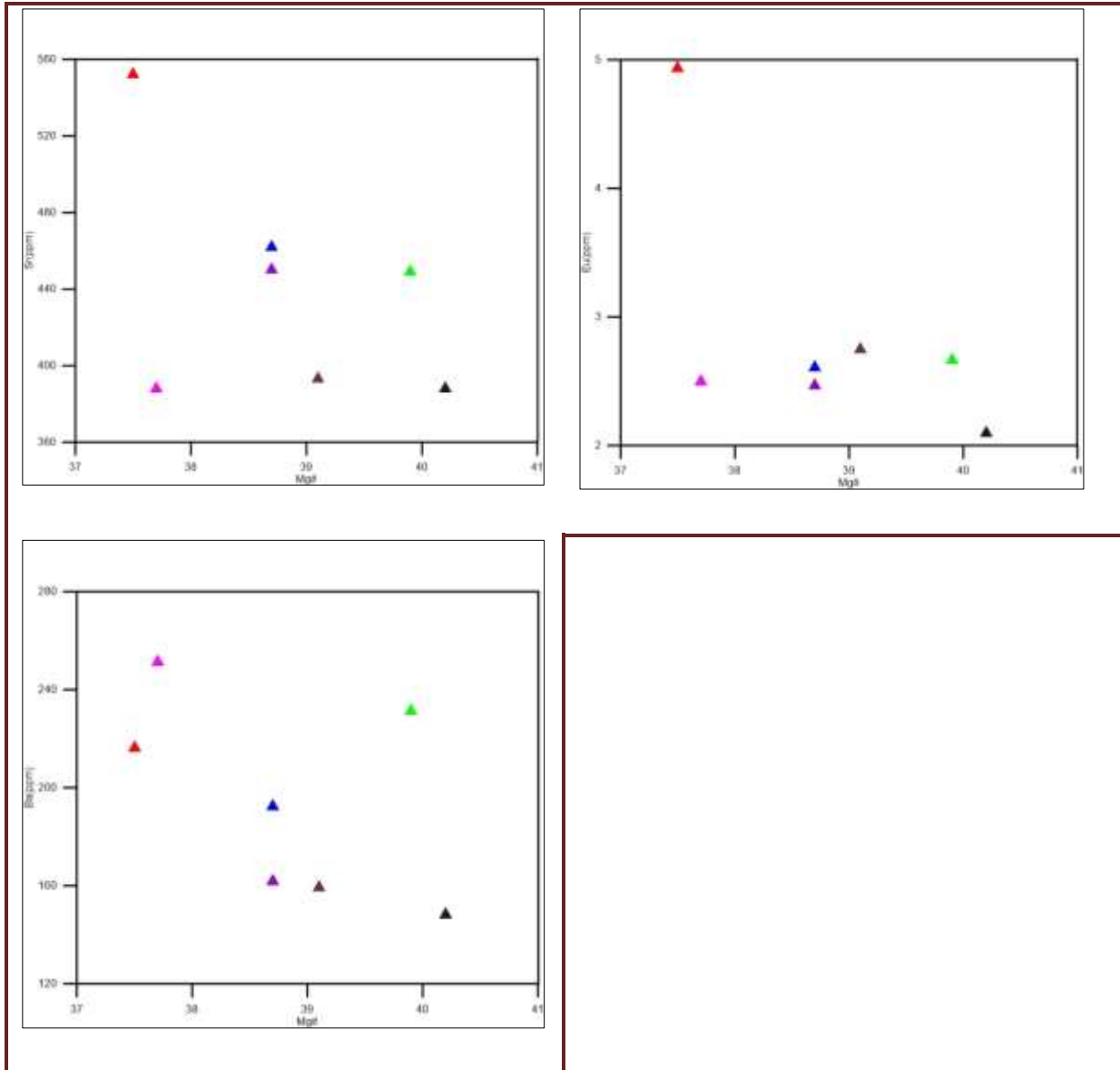


Figure.4.3. Variation diagrams of selected large ion lithophile (LIL) trace elements (ppm) as a function of Mg# content for analyzed Mertule Maryam area volcanic products (see legend fig 4.1).

Variation diagrams of HFSE (Zr, La, U, Th, Hf, Ta, Nb) plotted against Mg# (Fig4.4 below) shows scattered trend.

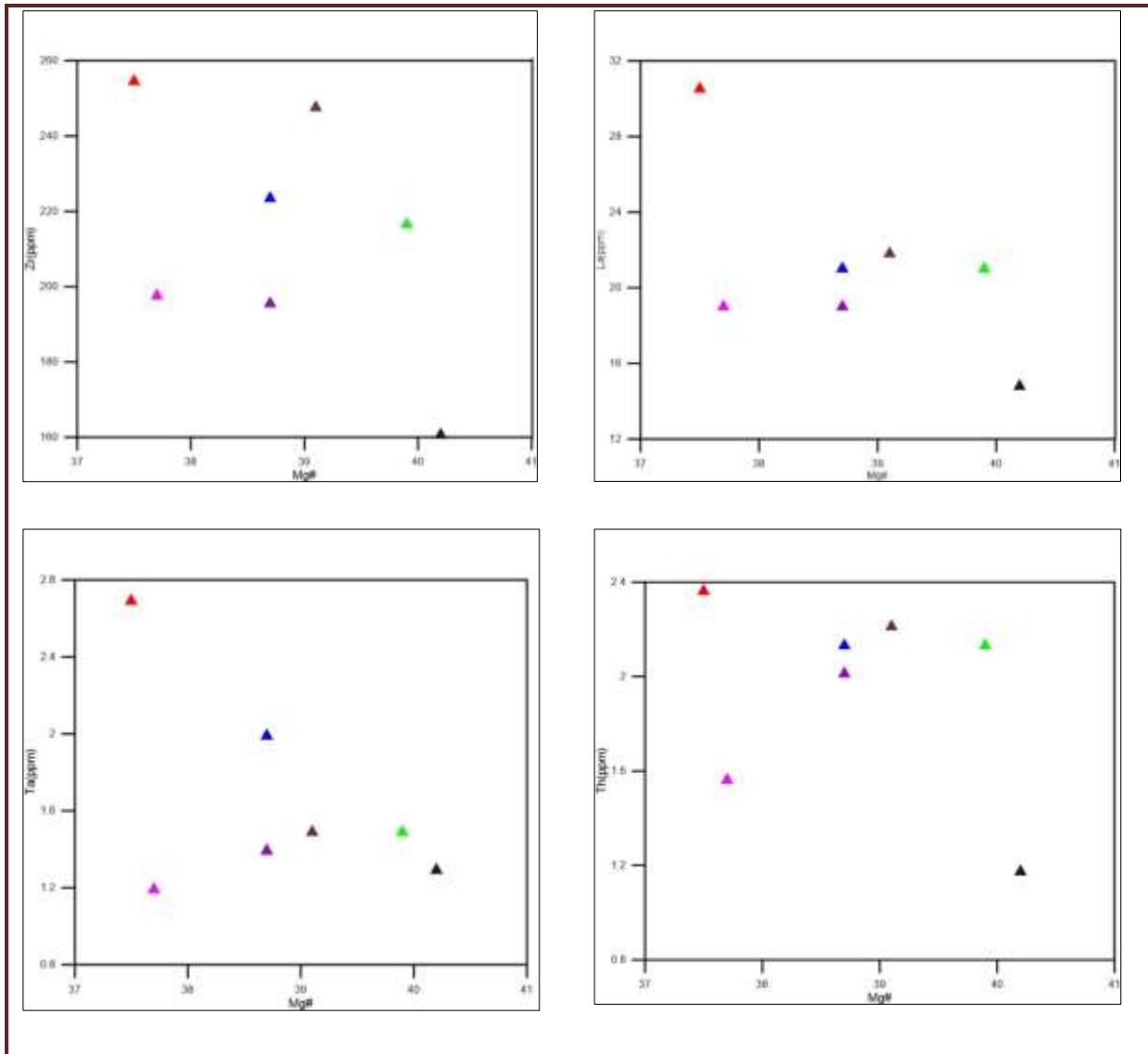


Figure.4.4. Variation diagrams of selected high field strength (HFS) trace elements (ppm) as a function of Mg# content for analyzed Mertule Maryam area volcanic products (see legend fig 4.1).

From the (Fig4.5 below) highly compatible elements (Ni, Co, Cr, and V) shows scattered trends. These samples have the following compatible element concentrations Ni: 9-94, Co: 17-45, Cr: 10 -150, and V: 191-425. These trace elements are exhibiting similar characteristics to accommodating major elements having strong scattered trends (e.g. Mg, Ca and Fe).

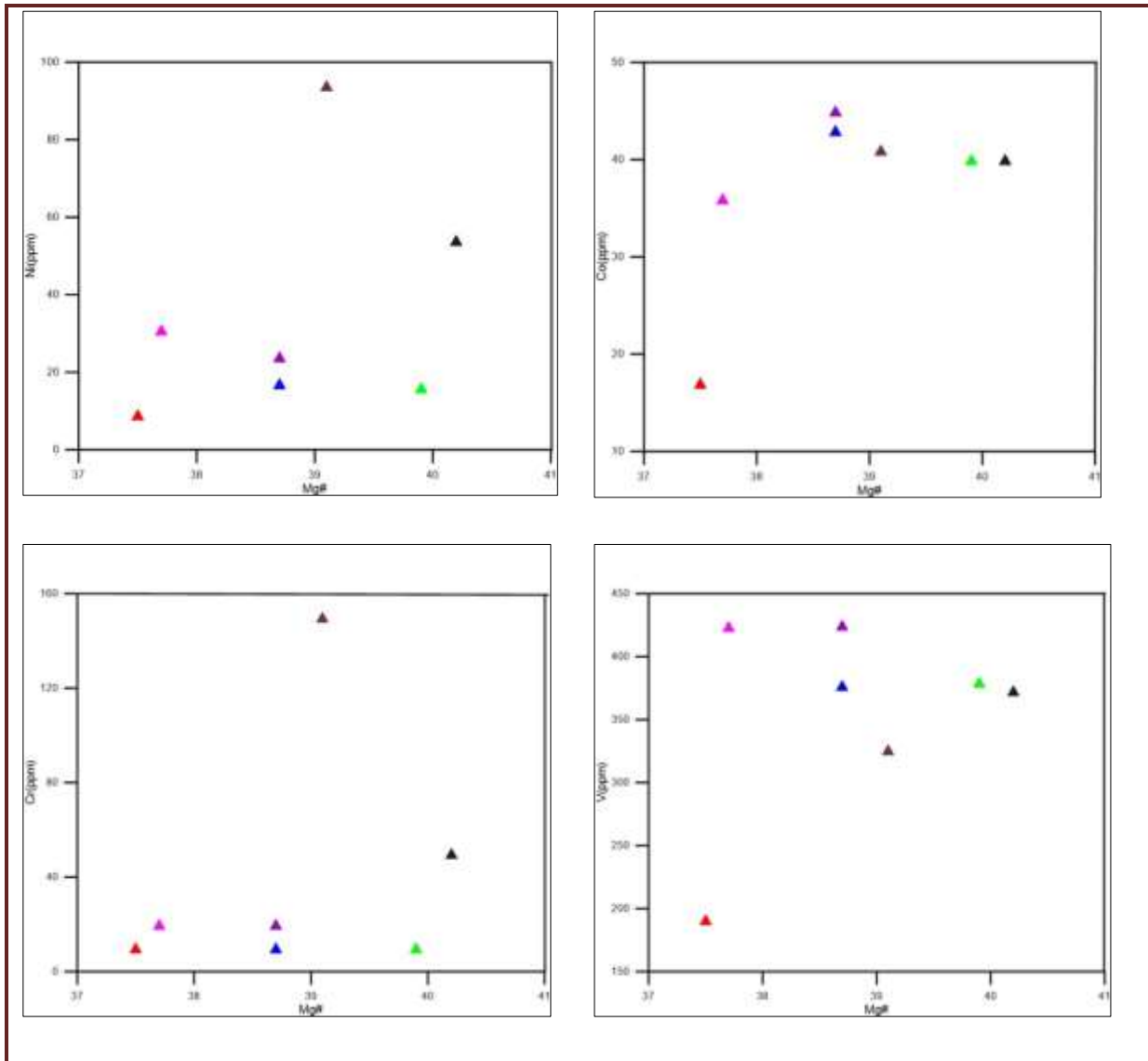


Figure.4.5. Variation diagrams for compatible trace elements (ppm) as a function of Mg# concentration (see legend fig 4.1).

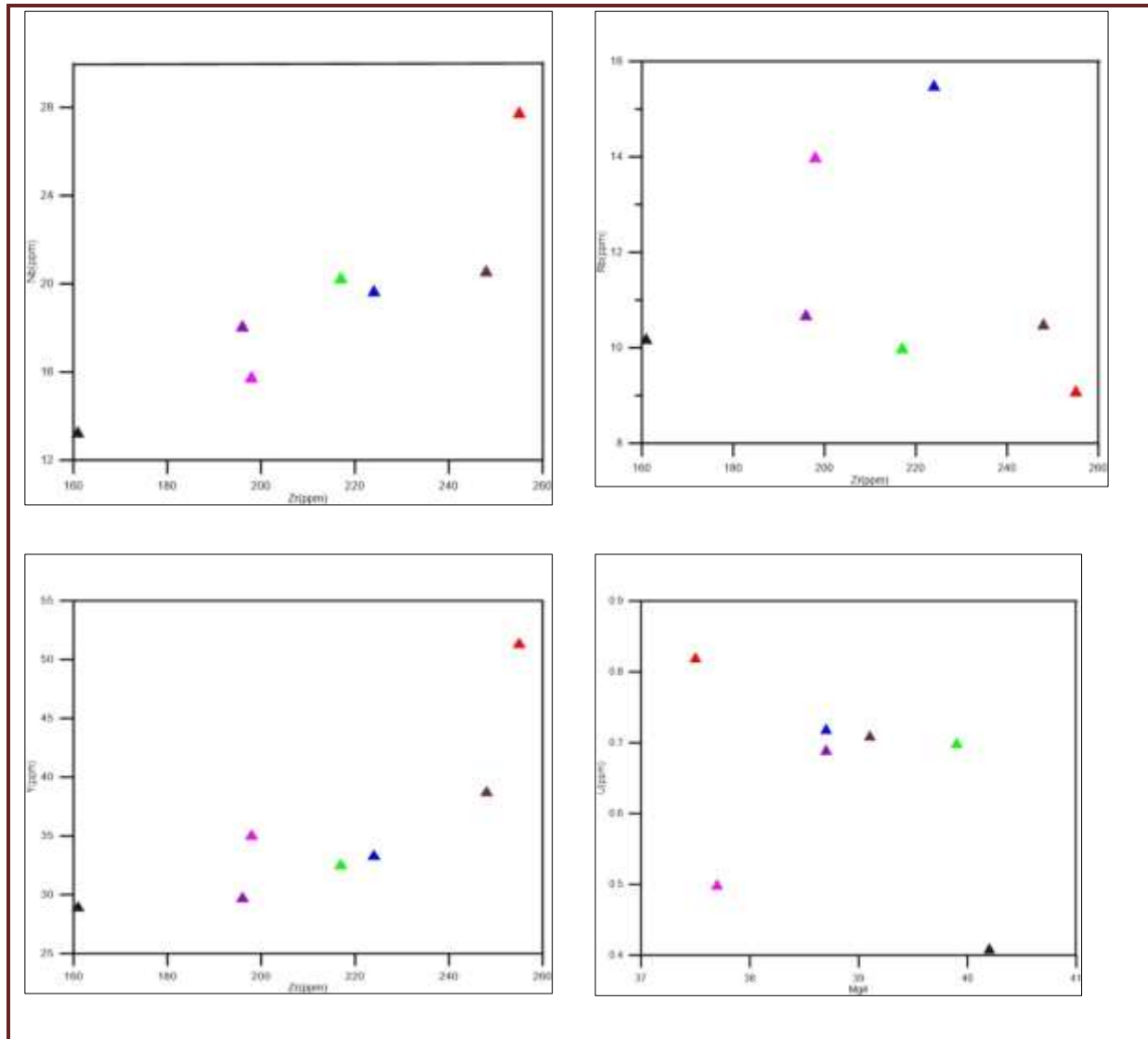


Figure.4.6. Variation diagrams for incompatible trace elements (ppm) as a function of Zr concentration expressed in (ppm) for Mertule Maryam area volcanic products (see legend fig 4.1).

Selected incompatible elements also plotted as a function of an incompatible element (Zr), showing scattered trend (Fig 4.5 above). Variation diagrams in Nb and Y as a function of Zr show slightly positive trends.

4.3. Chemical Spider diagrams

4.3.1. Rare earth element spider diagram

Rare earth element (REE) and trace element geochemical data for the analyzed rock samples are presented on a spider diagram based on their abundance and range of compatibility in the system of interest. REE abundance patterns for the representative analyzed samples are normalized by Chondrite values as shown in Fig.4.7 normalizing values are according to (COND- sun and McDonough 1989). In the spider diagram of REE, elements ordered with increasing compatibility from left to right (La to Lu). This rare earth element pattern provides information about the extent of crystallization and fractionation of magma.

The spider diagram of REE pattern indicates slightly flat slope in light rare earth element pattern (LREE) and almost flat heavy rare earth element pattern (HREE). The LREE is slightly enriched and HREE depleted relatively with about 10 times greater than the chondritic value.

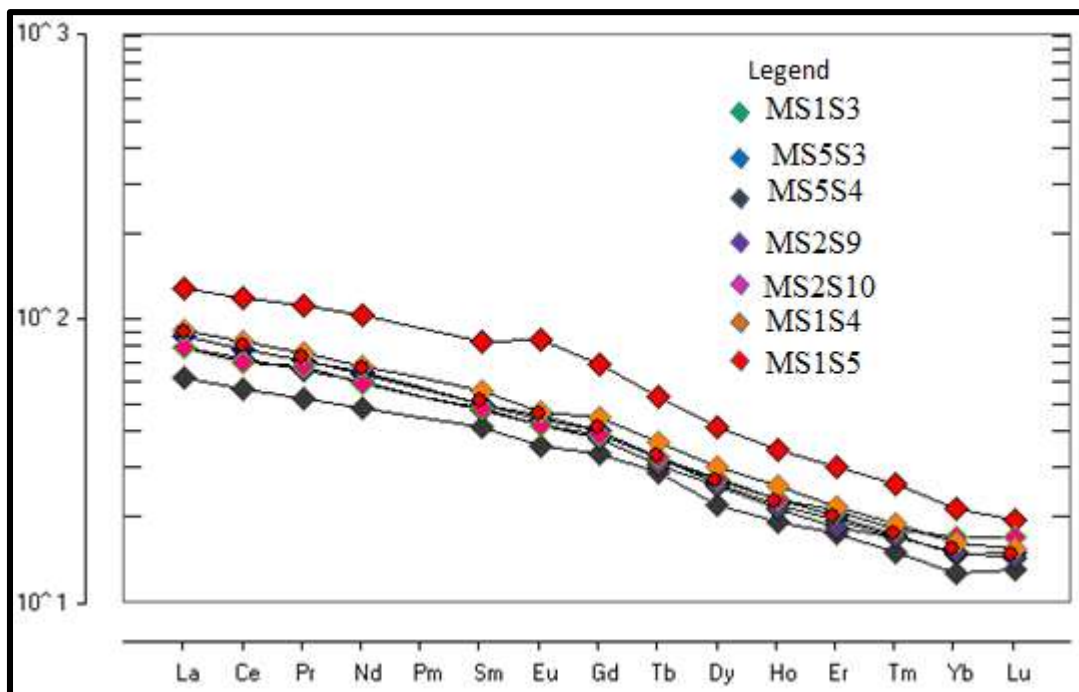


Figure.4.7, Spider diagrams of chondritic- normalized (COND- sun and McDonough 1989) Rare Earth element patterns of analyzed Mertule Maryam volcanic products.

4.3.2. Trace element spider diagram

The evolution of Mertule Maryam area volcanic products can also be understood from multi-element (Spider) diagrams constructed using primordial mantle (McDonough and sun 1995). The primitive mantle normalized incompatible trace element abundance profile (spider diagram) from Cs-Lu is shown in Fig 4.8. The spider diagram below shows slight enrichment in Ta and Pb and slight depletion Th, from the trace element spider plot presented in fig 4.8.

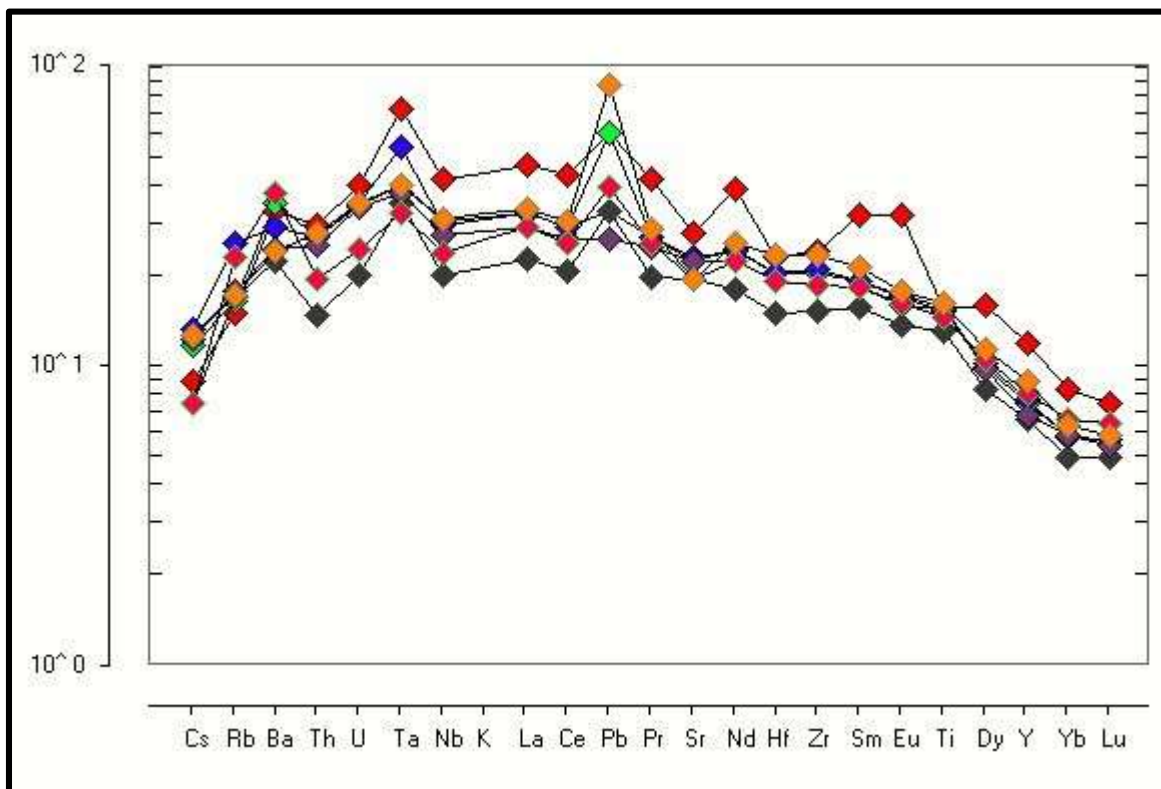


Figure.4.8. Spider plot for trace element patterns normalized to the primordial mantle (McDonough and sun 1995) analyzed samples from Mertule Maryam area volcanics (symbol as in fig 4.7).

CHAPTER FIVE

5. Discussion

The plateau of Ethiopia is separated by the MER into two segments as the northwestern and south-eastern Ethiopian plateau. The geology of the study is a part of the northwestern Ethiopia plateau, which belongs to the Oligocene flood basalt (Hoffmann et al., 1997; Kieffer et al., 2004). The research study mainly presents the geological map of the study area with geological cross-section and composite stratigraphic log section constructed based on field observation, petrographic analysis, and chemical composition. The petrographic investigation and geochemical analysis of selected samples with field observation are presented in this chapter. The combination of field observation and petrographic investigation shows; that the area is covered by mainly basalt, and patches agglomerate and tuff.

5.1. Petrography

Thin section was prepared and analyzed for Twenty-five fresh samples in terms of mineralogical assemblage, phenocryst assemblage and micro-texture with the help of field observation. Based on thin section analysis and field observation of hand specimen samples the study area is classified in to five units. To evaluate the magmatic process using petrography and stratigraphy first requires an assessment of parameters that control the crystallization of phases in basaltic magma. These parameters including (i) the starting composition of the parental magma, (ii) pressure of crystallization, and (iii) the presence of volatiles (Krans et al., 2018). The magma composition of the NW Ethiopian plateau is limited and classified into two based on the existing literature as LT and HT provinces, spatially restricted to the eastern and western half of the NW Ethiopian plateau, respectively (Pik et al., 1998; Kieffer et al., 2004; Beccaluva et al., 2009; Krans et al., 2018). From field observation and petrographic investigation, the flood basalts of the study area are classified into five units. The modal composition of samples analyzed for this study shows a range of mineral composition and textural features presented in chapter three. Rock units in this study constitute different mineral phases at phenocryst, microphenocryst and groundmass level having a different modal percentage. Pyroxene and plagioclase are the major phenocrysts and microphenocryst mineral phases identified from the analyzed rock samples. The mineralogical assemblage of (Pl+ CPx +Ol) suggests that fractionation occurred at a shallow

level in the upper crust. However mineralogical assemblages of (Ol+ Cpx) indicate that fractionation has occurred at a deeper level in the crust or at the crust-mantle boundary (Pik et al., 1998).

The crystallization of different minerals in rocks is used to understand the behavior of the magmatic system. In a relative dry magma, the crystallization of clinopyroxene at the expense of plagioclase and olivine is favored at high pressure (10-20 kbar), whereas plagioclase is crystallized over clinopyroxene at a lower pressure (<5kbar) in the same magma (Morse 1980; cited in Krans et al., 2018). In a relatively hydrated magma that contains water (>3wt %) clinopyroxene is crystallized over plagioclase at shallow crustal pressure (Feig et al., 2006). According to Kieffer et al. (2004) LT flood basalts are reported as dry; however, HT basalts have hydrated character with respect to the LT magmas (Beccaluva et al., 2009).

The analyzed volcanic rocks in the study area composed of minerals having different petrographic characteristics. The lower unit of the study area is plagioclase-pyroxene phyric that shows twinning in plagioclase and alteration effect in plagioclase and clinopyroxene, euhedral- subhedral- anhedral shapes are very common in the samples analyzed. The shape of the crystals imply the order of magma crystallization as euhedral to subhedral assumed to be crystallized first and anhedral crystallized later.

The plagioclase- pyroxene phyric basalt unit shows the mineral composition of phenocryst with a modal percentage of 10%-20% phenocrysts of plagioclase as the leading phase and followed by pyroxene and minor olivine. Plagioclase showing polysynthetic twinning, pikiolitic inclusion of clinopyroxene and sieved texture resulted from alteration. It is characterized by euhedral to subhedral shape, tabular and elongated phenocrysts are also observed from the analyzed samples with intergranular to microcrystalline groundmass. The pyroxene phenocrysts show subhedral shape, alteration effects are also observed. The groundmass constitutes of mafic minerals such as plagioclase laths, pyroxene, olivine and opaque minerals with intergranular texture. The most distinguishing feature observed in the lower flood basalt unit is the presence of plagioclase – pyroxene phyric flows. The mineral assemblage and the presence of plagioclase and clinopyroxene together suggest that they crystallized at considerable low pressure in the shallow crust rather than the mid-deep crust at considerable depth.

Agglomerate found overlain the lower basalt unit that shows rock fragments, feldspar crystals, calcite, and fine-grained groundmass. The feldspar crystals show sieve texture, calcites are filled within the vesicles of the rock fragments and between the rock fragments. This unit is found above the plagioclase- pyroxene phyric unit. A pause in flood basalt extrusion marked by 40 cm thick paleosols and about 3m thick tuff that indicates there was a gap in the eruption of the lava flow after the emplacement of the agglomerate. The paleosol represents weathering horizons of basalts or tuff during pauses in flood basaltic eruption. The pause suggests a decrease in magma flux; magma may still flux to the lithosphere, however the rate of fluxing to the lithosphere may not be high enough to cause the magma to erupt on the surface (Krans et al., 2018).

The aphyric basalt unit shows lava flows of different texture and field characteristics. The petrographic observation of different lava flows shows sparse plagioclase phenocryst and groundmass. The groundmass shows intergranular and trachytic flow texture. In addition, some samples show glomerocrysts of plagioclase in the microcrystalline groundmass. Samples taken from the sparsely porphyritic flow shows intergranular texture with plagioclase laths, opaque minerals, and fine mafic minerals are abundant in the groundmass. The modal mineralogical and textural observation of lava flows in this unit indicates that different fractionation nature than the overlain and the underlain basaltic units. The flows in this unit are thick with columnar jointed, and aphyric texture suggests an influx of magma into the plumbing system is high and the extrusion rate is high. The texture of this flood basalt unit is aphyric due to its high extrusion rate which could not allow the magma to settle in the shallow crust. This flood basalt unit indicates that there is no fractionation of different minerals in the shallow plumbing system. At the end of the aphyric basalt extrusion, there may be fractionation or melting of the crust due to the shallow magma chamber, which results in the formation of pyroclastic tuff. This indicates that at the end of the extrusion of the aphyric basalt there is a decrease in the influx of magma from the deeper staging chamber.

Samples analyzed from the plagioclase phyric basalt unit are consisting of columnar jointed, sparsely porphyritic and porphyritic basalts. The porphyritic flow composed of plagioclase phenocryst and poikilitic inclusion of pyroxene. The sparsely porphyritic unit shows subophitic texture between the plagioclase and pyroxene minerals. Petrographic investigations of lava flow samples taken from the columnar basalt shows glomerocrysts of plagioclase laths with microcrystalline groundmass. The sparsely porphyritic lava flow shows plagioclase

laths, olivine and opaque minerals with sub-ophitic and intergranular texture, with aphyric groundmass. The plagioclase phenocryst lava flow dominated with plagioclase phenocryst that shows polysynthetic twinning and zoning. It is characterized by euhedral to subhedral shape, tabular and elongated phenocrysts are also observed from the analyzed samples with intergranular to microcrystalline groundmass. The groundmass comprises plagioclase laths, opaque and fine-grained mafic minerals. It shows poikilitic inclusion of pyroxene enclosed by plagioclase phenocrysts. Modal observation of this unit shows plagioclase is the phenocryst phase devoid of pyroxene and olivine. The presence of plagioclase phenocryst indicates that the plagioclase is crystallized at low pressure in the shallow crust. This suggests that there is a decrease in magma recharge into the plumbing system that produces the plagioclase phenocryst flood basalt unit.

The modal percentage of undifferentiated aphyric basalt unit shows identifiable plagioclase, opaque and groundmass. This flood basalt unit is columnar jointed and intercalated with pyroclastic tuff. Modal mineralogy and texture of analyzed samples from this flood basalt unit suggests that there is different fractionation history. The influx rate of magma to the plumbing system is high and the extrusion rate is high due to this reason the magma could not have a long residence time in the shallow crust to form any crystal which is identifiable from hand specimen sample and petrographic observation. Tuff may be formed due to shallow fractionation of magma or it may be from melt generated from the crust due to the magma chamber in the shallow crust, when there is a decrease in the flux of magma into the magma chamber and if there is long residence time in the crust. The longer residence time of magma results in the fractionation of mafic minerals and resulted in the formation of the felsic volcanic product.

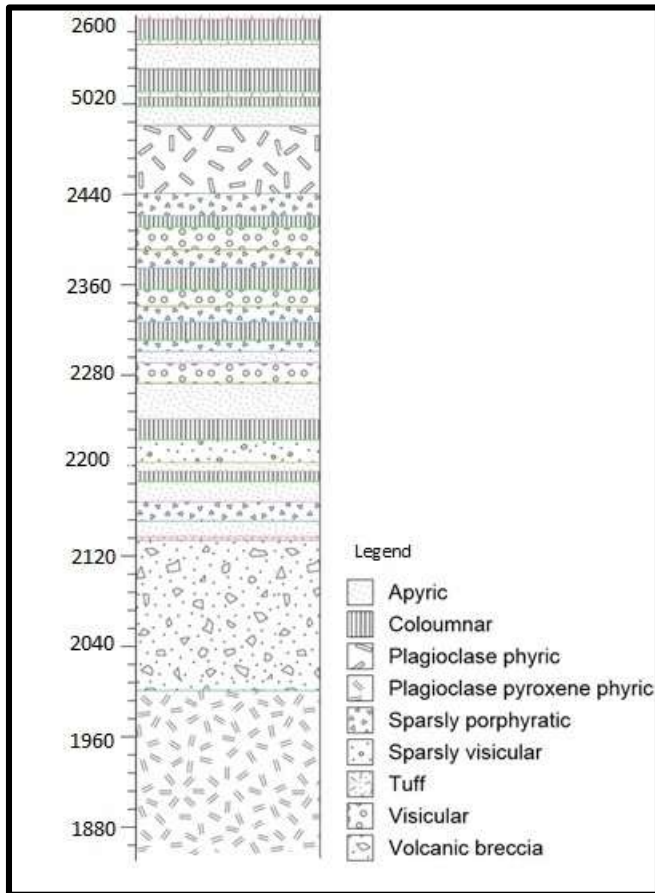


Figure 5.1. Petrostratigraphy of Mertule Maryam area volcanic products

5.2. CIPW Normative minerals of Mertule Maryam volcanics

CIPW normative minerals determined from major geochemical analysis have been associated with petrographic descriptions and interpretation obtained from Mertule Maryam area volcanics. The petrographic modal composition taking only visible phenocryst mineral phases whereas, CIPW calculations take the wt% of major oxides for mineral phase at groundmass and phenocryst level. Normative mineral abundance is the calculated wt% of particular mineral; excluding hydrous minerals in the calculation. The normative data of analyzed rocks presented in chapter four (table 4.1), show that Mertule Maryam area basalts are Hypersthene normative (12.06-9.86 wt %) and contain normative of quartz (7.63-4.54 wt %). The presence of hypersthene and quartz in the norm can justify Mertule Maryam area basalts classified as silica saturated rocks.

5.3. Petrogenetic indicators

In Total alkali-silica (TAS) classification diagram in chapter four (Fig4.1) shows, all the analyzed samples fall in the region of basalt compositional field based on $\text{Na}_2\text{O} + \text{K}_2\text{O}$ versus SiO_2 content.

Different scattered trend are observed from major element versus Mg#, trace versus Mg# content, and trace versus trace. Additionally, spider diagrams of Chondritic normalized REE and primordial mantle-normalized trace elements and other combinations used and interpreted following their signature. Trace element ratios also thoroughly used to explain the petrogenesis of analyzed rocks. In Fig 4.2 selected major oxides are plotted against Mg# for Mertule Maryam area mafic samples. Most of the plots of major oxides show scattered nature that indicates these volcanic products are not the result of simple fractionation.

To understand whether the rock is sourced from primary magma or not, it is tested by MgO, Ni, and Cr concentration. Parent magma is characterized by a high concentration of (Ni :> 400-500ppm, Cr :> 1000 ppm, and MgO: 10 -15wt%, (Frey et al., 1978; Hess, 1992 as cited in Dereje Ayalew et al., 2016). In addition to this parent magma is derived from high-temperature have small melt fraction and this melt is characterized with high concentration of MgO: 15-16%, and TiO_2 : 3-7% (Rogers et al., 2010). Rocks of the present study show a distinctly lower concentration of MgO: 4.17 – 4.82%, TiO_2 : 2.63-3.3%, Ni: 9-94, Cr: 10 -150 ppm. Hence, the magma that resulted in basalts of the study area undergoes olivine and clinopyroxene fractionation.

Variation diagrams plotted for trace element against Mg# and trace element against trace element shows scattered pattern suggested the presence of more than one magmatic lineage. The analyzed mafic rocks in the study area have a low concentration of compatible trace element $\text{Ni} < 94$ and $\text{Cr} < 150$ showing fractionation of olivine and clinopyroxene. The ratio of highly incompatible trace element Zr/Nb (9.2-12.53), Hf/La (0.22-0.31), and Zr/Ce (3.5-4.8) vary within the analyzed rocks. The variation in these trace elements will not vary in the course of fractional crystallization and the variation may reflect source heterogeneity (Dereje Ayalew., 1999).

Variation diagrams of selected major oxides plotted against Mg# such as TiO_2 , CaO, Na_2O and P_2O_5 show scattered trend. Generally, the major oxide variation diagram shows scattered

trend due to accumulation and fractionation of heterogeneous phenocrysts or the result of different ways of movement in the crust.

Variation diagrams constructed using high field strength elements (HFS) Nb, Th, Y, Hf, against Zr shows scattered trend. This can be justified as the derivation of analyzed basaltic samples is from a different plumbing system.

REE pattern of Mertule Maryam area flood basalt samples is shown in figure 4.7. In this figure, basalt samples show relative enrichment in light rare earth element (LREE) and flat pattern in heavy rare earth element (HREE). The relative enrichment in light rare earth element (LREE) suggests that the examined basaltic samples are sourced from the enriched mantle and there is significant involvement of contaminating crustal materials which can enhance the enrichment of LREE and highly incompatible trace elements (Dereje Ayalew et al., 1999; 2016). The Chondrite-normalized REE pattern of the Mertule Maryam area basaltic lava samples (fig 4.7,) show slight REE enrichment, especially in the LEER (La/Yb 6.5- 8.3), and they have flat heavy REE patterns. There is no lava that showing a significant anomaly in Eu ($Eu/Eu^* = 0.93-1.09$). Both LREE and HREE are enriched (>10 times) than Chondritic value (Fig. 4.7) with the distinctly varying trend as relatively steep for LREE and flat for HREE, implying spinel/garnet free source. The basalts of the study area are characterized by low CaO/Al₂O₃ ratios (0.58–0.72) and flat HREE patterns ($Tbn/Ybn = 0.42-0.54$) together with somewhat elevated HREE concentrations higher than 10-times chondritic values which most likely suggest a mantle source containing spinel rather than garnet(Dereje Ayalew.,2016).

The continental crust is enriched in Pb and Ba, whereas Ta, Nb, and Ti are depleted (Pik et al., 1999). Trace element spider diagrams (Fig. 4.8) normalized to the primordial mantle of McDonough and sun (1995) presented in chapter four (Fig. 4.8), show basaltic samples exhibiting enrichment in Ta and Pb. Ta and Pb exhibit slight enrichment indicative of the presence of crustal contamination during magma emplacement to surface. The OIB and MORB mantles have high and relatively constant Ce/Pb (25 ± 5), whereas the upper crust has much lower ratios (Hofmann et al. 1986; cited in Shinjo et al.,2011), hence basaltic samples of the study area shows Ce/Pb ratios of 3.9-11 shows crustal contamination during emplacement of magma.

CHAPTER SIX

6. Conclusion and Recommendation

6.1. Conclusions

Northwestern Ethiopia is characterized by extensive flood basalt overlain by the shield and Quaternary volcanic products. The flood basalts of this volcanic province are subdivided into two based on the titanium concentration: high-titanium (HT) and low-titanium (LT) (Pik et al., 1998). The study area is situated in the NW Ethiopian plateau, which fall in the HT province. A combination of field observation, petrographic study, geochemical data and reviews of regional previous works provide new insight into the evolution of the magmatic plumbing system of continental flood basalts (CFB) of the study area. The major findings from the present study are as follows:

- From the petro-stratigraphic observation of the analyzed samples the study area is classified into three plagioclase-pyroxene phyric, aphyric and plagioclase phyric separated with paleosol and pyroclastic tuff that indicates hiatus in eruption. This suggests initial flows are fed by magmas that experienced deeper fractionation (mid to deep crust). Correspondingly, overtime the fractionation become polybaric thus reflecting the settling of magma in both shallow and deep crust.
- The volcanic products in the study area are basalts, from the petrographic and geochemical analysis. It shows narrow compositional variations as (47-51 wt% silica content). In addition, pyroclastic tuff is exposed in the study area from field observation.
- The plagioclase – pyroxene basalt indicates there was considerable depth of fractionation in the shallow plumbing system. The aphyric basalt indicates that the deep fractionated magma is not settled in the shallow crust. This is due to the maturity of the conduit allows the influx of magma from the chamber to the plumbing system is high and the extrusion rate is high. The plagioclase phyric unit is characterized by large tabular plagioclase phenocryst that shows polysynthetic twinning and zoning. From the petrographic observation, the magma that produces this unit is subjected to shallow crust fractionation of deeper fractionated magma. It has enough time in the shallow crust to settle and produce plagioclase phenocryst. The influx of magma to the shallow plumbing system decreases resulting in the formation of plagioclase phenocryst with microphenocrysts of mafic minerals.

6.2. Recommendations

The Mertule Maryam area requires further detail investigation:

- Further studies by increasing the amount of sampling and field techniques to map the non-accessible areas
- Isotopic geochemistry required to understand the evolution and geochronologic history in addition to the petrographic and geochemical analysis
- Studies on the mineral chemistry are also required to determine the qualitative and quantitative mineral composition of volcanic rock units.

REFERENCES

- Abbate, E., Bruni, P., & Sagri, M. (2015). Geology of Ethiopia: a review and geomorphological perspectives. In *Landscapes and landforms of Ethiopia* (pp. 33-64). Springer, Dordrecht.
- Addise Mekonnen (2006). Geology and Geochemistry of Guna Volcanic Massif, North western Ethiopian plateau. Unpublished MSc Thesis, Addis Ababa University, Addis Ababa, Ethiopia, 100 pp.
- Asfawossen, Asrat., Barbey, P., & Gleizes, G. (2001). The Precambrian geology of Ethiopia: a review. *Africa Geoscience Review*, **8**(3/4):271-288.
- Baker, J., Snee, L., & Menzies, M. (1996). A brief Oligocene period of flood volcanism in Yemen: implications for the duration and rate of continental flood volcanism at the Afro-Arabian triple junction. *Earth and Planetary Science Letters*, **138**(1-4): 39-55.
- Beccaluva, L., Bianchini, G., Natali, C., & Siena, F. (2009). Continental flood basalts and mantle plumes: a case study of the Northern Ethiopian Plateau. *Journal of Petrology*, **50**(7): 1377-1403.
- Bekele, Abebe., Acocella, V., Tesfay,Korme., & Dereje, Ayalew. (2007). Quaternary faulting and volcanism in the Main Ethiopian Rift. *Journal of African Earth Sciences*, **48**(2-3): 115-124.
- Berhe, S. M., Desta, B., Nicoletti, M., & Teferra, M. (1987). Geology, geochronology and geodynamic implications of the Cenozoic magmatic province in W and SE Ethiopia. *Journal of the Geological Society*, **144**(2): 213-226.
- Boccaletti, M., Bonini, M., Mazzuoli, R., Abebe, B., Piccardi, L., & Tortorici, L. (1998). Quaternary oblique extensional tectonics in the Ethiopian Rift (Horn of Africa). *Tectonophysics*, **287**(1-4): 97-116.
- Corti, G. (2009). Continental rift evolution: from rift initiation to incipient break-up in the Main Ethiopian Rift, East Africa. *Earth-science reviews*, **96**(1-2): 1-53.
- Coulié, E. (2001). Chronologie $^{40}\text{Ar}/^{39}\text{Ar}$ et K/Ar de la dislocation du plateau éthiopien et de la déchirure continentale à la corne de l'Afrique depuis 30 Ma (Doctoral dissertation, Paris 11).

- Chorowicz, J. (2005). The East African rift system. *Journal of African Earth Sciences* **43**: 379-410.
- Daniel, Meshesha., & Shinjo, R. (2007). Crustal contamination and diversity of magma sources in the northwestern Ethiopian volcanic province. *Journal of Mineralogical and Petrological Sciences*, 0706050032-0706050032.
- Davaille, A. and Vatteville, J. (2005). On the transient nature of mantle plume. *Geophysical Research Letters* **32**: 1- 4.
- Dereje, Ayalew. & Gibson, S. A. (2009). Head-to-tail transition of the Afar mantle plume: Geochemical evidence from a Miocene bimodal basalt–rhyolite succession in the Ethiopian Large Igneous Province. *Lithos*, **112**(3-4): 461-476.
- Dereje, Ayalew. Jung, S., Romer, R. L., Kersten, F., Pfänder, J. A., & Garbe-Schönberg, D. (2016). Petrogenesis and origin of modern Ethiopian rift basalts: Constraints from isotope and trace element geochemistry. *Lithos*, **258**:1-14.
- Dereje, Ayalew., Barbey, P., Marty, B., Reisberg, L., Yirgu, G., & Pik, R. (2002), Source, genesis, and timing of giant ignimbrite deposits associated with Ethiopian continental flood basalts. *Geochimica et Cosmochimica Acta*, **66**(8): 1429 – 1448.
- Dereje, Ayalew., Gezahegn, Yirg., & Pik, R., (1999), Geochemical and isotopic (Sr, Nd and Pb) characteristics of volcanic rocks from southwestern Ethiopia. *Journal of African earth sciences*, **29**(2):38 – 391.
- Dereje, Ayalew and Gezahegn, Yirgu . (2003), crustal contribution to the genesis of Ethiopian Plateau rhyolitic ignimbrites, basalt and rhyolite geochemical provinciality. *Journal of the Geological society*, **160**: 47-56.
- Ebinger, C. J., & Sleep, N. H. (1998). Cenozoic magmatism throughout east Africa resulting from impact of a single plume. *Nature*, **395**(6704): 788-791.
- Ebinger, C. J., Yemane, T., Woldegabriel, G., Aronson, J. L., & Walter, R. C. (1993). Late Eocene–Recent volcanism and faulting in the southern main Ethiopian rift. *Journal of the Geological Society*, **150**(1): 99-108.
- Feig, S. T., Koepke, J. and Snow, J. E. (2006). Effect of water on tholeiitic basalt phase equilibria: an experimental study under oxidizing conditions. *Contributions to Mineralogy and Petrology*, **152**(5):611-638.
- Ferede Chumburo (2015). Geology of Debre Markos Map Sheet (NC 37-6). Memoir No. 27. Geological Survey of Ethiopia. 87 p.

- Feyissa Dejene Hailemariam, (2018). Petrologic and geochemical evidence for diversity of magma compositions at the Ethiopian volcanic province: implications for thermo-chemical plume influence.
- Furman, T., Kaleta, K. M., Bryce, J. G., & Hanan, B. B. (2006). Tertiary mafic lavas of Turkana, Kenya: constraints on East African plume structure and the occurrence of high- μ volcanism in Africa. *Journal of Petrology*, **47**(6): 1221-1244.
- Furman, T., Nelson, W. R., & Elkins-Tanton, L. T. (2016). Evolution of the East African rift: Drip magmatism, lithospheric thinning and mafic volcanism. *Geochimica et Cosmochimica Acta*, **185**:418-434.
- George, R., Rogers, N., & Kelley, S. (1998). Earliest magmatism in Ethiopia: Evidence for two mantle plumes in one flood basalt province. *Geology*, **26**(10): 923-926.
- Gezahegn, Yirgu. (1997). Magma – crust interaction during emplacement of Cenozoic volcanism in Ethiopia: geochemical evidence from Sheno-Megezez area, central Ethiopia. *SINET: Ethiop. J. Sc.* **20**(1): 49-72 pp.
- Gezahegn, Yirgu., Ebinger, C. J. & Maguire, P. K. H. (2006). The Afar Volcanic Province within the East African Rift System. Geological Society, London, Special Publications **259**, 327 pp.
- Hofmann AW, Jochum KP, Seuffer M, White WM (1986) Nb and Pb in oceanic basalts: new constraints on mantle evolution. *Earth Planet Sci Lett* **79**:33–45.
- Hofmann, C., Courtillot, V., Feraud, G., Rochette, P., Gezahegn, Yirgu. Ketefo, E., & Pik, R. (1997). Timing of the Ethiopian flood basalt event and implications for plume birth and global change. *Nature*, **389**(6653), 838.
- <https://en.climate-data.org/location/928327/> accessed on 18.03.2019
- Kieffer, B., Nicholas, A., Henriette, L., Florenece, B., Delphine, B., Arnaud, P., Gezahegn, Yirgu., Dereje, Ayalew., Dominique, W., Dougal, A.J., Francine, K., and Claudine, M. (2004). Flood and shield Basalt from Ethiopia magmas from the African superswell *Journal of petrology* **45**:793-834.
- Krans, S. R., Rooney, T. O., Kappelman, J., Gezahegn, Yirgu., & Dereje, Ayalew. (2018). From initiation to termination: a petrostratigraphic tour of the Ethiopian Low-Ti Flood Basalt Province. *Contributions to Mineralogy and Petrology*, **173**(5), 37.

- Le Bas, M. J., Le Maitre, R., Streckeisen, A. and Zanettin, B. (1986). A chemical classification of volcanic rocks based on the total alkali-silica diagram. *Journal of Petrology* **27**(3):745- 750.
- McDonough, W. F. and Sun, S.S. (1995). The composition of the Earth. *Chemical Geology* **120**(3):223-253.
- Mengesha, Tefera., Tadiwos, Chernet., & Haro, W., (1996). Explanation of the Geological Map of Ethiopia. *Ethiopian Geological Surveys, Bull.*, **3**: 80p.
- Mohor, p. 1962. The Ethiopian rift system. *Bulletin of the Geophysical Observatory, Addis Ababa*, **3**, 33 – 62.
- Mohr, P. 1983. Ethiopian flood basalt province. *Nature*, **303**, 577 – 584.
- Mohr, P., & Zanettin, B. (1988). The Ethiopian flood basalt province. In *Continental flood basalts* (pp. 63-110). Springer, Dordrecht.
- Peccerillo, A., Barberio, M. R., Gezahgn, Yirgu., Dereje, Ayalew., Barbieri, M. W. U. T. W., & Wu, T. W. (2003). Relationships between mafic and peralkaline silicic magmatism in continental rift settings: a petrological, geochemical and isotopic study of the Gedemsa volcano, central Ethiopian rift. *Journal of Petrology*, **44**(11): 2003-2032.
- Pik, R., Deniel, C., Coulon, C., Gezahgn, Yirgu., Hofmann, C., & Dereje, Ayalew. (1998). The northwestern Ethiopian Plateau flood basalts: classification and spatial distribution of magma types. *Journal of Volcanology and Geothermal Research*, **81**(1-2): 91-111.
- Pik, R., Deniel, C., Coulon, C., Gezahgn, Yirgu., & Marty, B. (1999). Isotopic and trace element signatures of Ethiopian flood basalts: evidence for plume–lithosphere interactions. *Geochimica et Cosmochimica Acta*, **63**(15): 2263-2279.
- Rogers, N. W., Davies, M. K., Parkinson, I. J., & Yirgu, G. (2010). Osmium isotopes and Fe/Mn ratios in Ti-rich picritic basalts from the Ethiopian flood basalt province: No evidence for core contribution to the Afar plume. *Earth and Planetary Science Letters*, **296**(3-4): 413-422.
- Rogers, N., Macdonald, R., Fitton, J. G., George, R., Smith, M., & Barreiro, B. (2000). Two mantle plumes beneath the East African rift system: Sr, Nd and Pb isotope evidence from Kenya Rift basalts. *Earth and Planetary Science Letters*, **176**(3-4): 387-400.

- Rooney, T. O. (2017). The Cenozoic magmatism of East-Africa: Part I—flood basalts and pulsed magmatism. *Lithos*, **286**: 264-301.
- Shinjo, R., Chekol, T., Meshesha, D., Itaya, T., & Tatsumi, Y. (2011). Geochemistry and geochronology of the mafic lavas from the southeastern Ethiopian rift (the East African Rift System): assessment of models on magma sources, plume–lithosphere interaction and plume evolution. *Contributions to Mineralogy and Petrology*, **162**(1): 209-230.
- Sun, S. S. and McDonough, W. F. (1989). Chemical and systematic of oceanic basalts: implications for mantle composition and processes. In: Saunders, A. D. and Norry, M. J. (eds) *Magmatism in the ocean Basins*, Geological Society, London. Special publications **42**: 313-347.
- Tsegaye Abebe, Mazzarini, F., Innocenti, F. and Manetti, P. (1998). The Yerer-Tullu Wellel volcanotectonic lineament: A transtensional structure in central Ethiopia and the associated magmatic activity. *Journal of African Earth Sciences* **26**(1):135-150.
- Ukstins, I. A., Renne, P. R., Wolfenden, E., Baker, J., Ayalew, D., & Menzies, M. (2002). Matching conjugate volcanic rifted margins: $^{40}\text{Ar}/^{39}\text{Ar}$ chrono-stratigraphy of pre-and syn-rift bimodal flood volcanism in Ethiopia and Yemen. *Earth and Planetary Science Letters*, **198**(3-4): 289-306.
- Williams .F.M2016, *Understanding Ethiopia*, Springer International Publishing, Switzerland.
- Zanettin, B., Justin-Visentin, E., Nicolrtti, M., and Piccirillo, E.M. 1980. Correlations among Ethiopian volcanic formations with special references to the chronological and stratigraphical problems of the “Trap Series” *Atti dei Convegni Lincei*, **47**: 231-252.

APPENDIX-A: Petrographic analysis results

Sample	Rock type	Average modal proportion (%)		Average grain shape
MS1S1	Porphyritic basalt lava flow	Plagioclase	6%	Euhedral – subhedral tabular form
		Pyroxene	4%	Anhedral
		Olivine	1%	Anhedral
		Opaque	8%	Anhedral
		Groundmass	79%	Microcrystalline
MS4S1	Porphyritic basaltic lava flow	Plagioclase	12%	Euhedral – sub hedral
		Pyroxene	8%	Subhedral-anhedral
		Opaque	5%	Anhedral
		Groundmass	75%	Anhedral
MS1S2	Agglomerate	Rock fragment	25%	Anhedral
		Infilling material	8%	-
		Feldspar	1-2%	Anhedral
		Groundmass	65%	Anhedral
MS4S3		Rock fragment	20%	Anhedral
		Infilling material	10%	-
		Groundmass	70%	-
MS1S3	Aphyric	Opaque	10%	Anhedral
		Groundmass	90%	Cryptocrystalline
MS1S4	Aphyric	Plagioclase laths	10%	anhedral

		Groundmass	90%	Microcrystalline
MS1S5	Aphyric	plagioclase	2%	Subhedral
		Groundmass	98%	Anhedral
MS2S6		Plagioclase lath	2%	anhedral
		groundmass	98%	anhedral
MS2S1		Plagioclase lath	2%	Anhedra
		Ground mass	98%	Microcrystalline
MS2S9	Sparsely porphyritic	Plagioclase	3%	Anhedral
		Groundmass	97%	Microcrystalline
MS5S1	Plagioclase phytic basalt	plagioclase	30%	Euhedral – subhedral tabular form
		Groundmass	70%	Microcrystalline
MS5S2	Plagioclase phytic basalt	Plagioclase	10%	Euhedral – subhedral tabular form
		Opaque	5%	Anhedral
		Groundmass	85%	Microcrystalline
MS5S3	Aphyric basalt	Plagioclase	2%	Subhedral
		Opaque	8%	Anhedral
		Groundmass	90%	Microcrystalline
MS5S4	Aphyric basalt	groundmass		Microcrystalline
MD1	Dike	Pyroxene	3%	anhedral
		Opaque	2%	Anhedral
		Groundmass	95%	Microcrystalline

APPENDIX-B: Selected trace element ratio of analyzed samples

Sample	Ce/Pb	Zr/Ce	CaO/Al ₂ O ₃	Lan/Ybn	Tb/Yb	Nb/U	Hf/La	Zr/Nb	La/Nb
MS1S5	8.14444 4	3.47885 4	0.584328	8.27027	0.54324 3	33.9024 4	0.21568 6	9.17266 2	1.10071 9
MS1S3	5.43333 3	4.43762 8	0.640727	8.11538 5	0.47307 7	29	0.27488 2	10.6896 6	1.03940 9
MS5S3	9.78	4.58077 7	0.634432	8.17829 5	0.47674 4	27.3611 1	0.27488 2	11.3705 6	1.07106 6
MS5S3	7	4.6	0.72342	6.77272 7	0.5	32.4390 2	0.28859 1	12.1052 6	1.12030 1
MS2S9	11.175	4.38478 7	0.675277	7.31800 8	0.44444 4	26.2318 8	0.28795 8	10.8287 3	1.05524 9
MS2S10	7.26666 7	4.54128 4	0.641045	6.47457 6	0.41694 9	31.6	0.28795 8	12.5316 5	1.20886 1
MS4S1	3.95384 6	4.82490 3	0.658993	7.73851 6	0.49116 6	29.0140 8	0.30593 6	12.0388 3	1.06310 7
La/Yb	Dy/Yb	Rb/Nb	Th/Ta	Th/La	Ba/La	La/Y	La/Nb	Ba/Nb	Ba/Th
8.27027	2.91891 9	0.32733 8	8.917137	0.03670 9	7.09150 3	0.59533 1	1.10071 9	7.80575 5	91.5611 8
8.11538 5	2.61153 8	0.49261 1	5.301423	0.09292	10.9952 6	0.64723 9	1.03940 9	11.4285 7	108.411 2
8.17829 5	2.69379 8	0.78680 2	3.423731	0.22980 8	9.14691 9	0.63173 7	1.07106 6	9.79695 4	90.1869 2
6.77272 7	2.59545 5	0.76691 7	3.384269	0.22661 2	10	0.51379 3	1.12030 1	11.2030 1	126.271 2
7.31800 8	2.54789 3	0.59116	4.309987	0.13716 1	8.50785 3	0.64094	1.05524 9	8.97790 1	80.4455 4
6.47457 6	2.41694 9	0.88607 6	2.7277	0.32484 4	13.1937 2	0.54416	1.20886 1	15.9493 7	160.509 6
7.73851 6	2.73498 2	0.50970 9	5.365775	0.09499 3	7.30593 6	0.56443 3	1.06310 7	7.76699	72.0720 7